Synthesis, vibrational spectroscopy and X-ray structural characterization of novel NIR emitter squaramides

Marina Ávila-Costa, Claudio L. Donnici, Jordana Dias dos Santos, Renata Diniz, Alexandre Barros Barbosa, Alexandre Cuin, Luiz Fernando Cappa de Oliveira

PII:	S1386-1425(19)30744-9
DOI:	https://doi.org/10.1016/j.saa.2019.117354
Article Number:	117354
Reference:	SAA 117354
To appear in:	*Spectrochimica Acta Part A: Molecular and Biomolecular Spectroscopy*
Received date:	11 April 2019
Revised date:	2 July 2019
Accepted date:	7 July 2019

Please cite this article as: M. Ávila-Costa, C.L. Donnici, J.D. dos Santos, et al., Synthesis, vibrational spectroscopy and X-ray structural characterization of novel NIR emitter squaramides, Spectrochimica Acta Part A: Molecular and Biomolecular Spectroscopy, https://doi.org/10.1016/j.saa.2019.117354

Synthesis, vibrational spectroscopy and X-ray structural characterization of novel NIR emitter squaramides

Marina Ávila-Costa[a], Claudio L. Donnici[a,*], Jordana Dias dos Santos[b], Renata Diniz[a], Alexandre Barros Barbosa[a], Alexandre Cuin[b], Luiz Fernando Cappa de Oliveira[b],

[a] Departamento de Química, Instituto de Ciências Exatas, Universidade Federal de Minas Gerais, Belo Horizonte, MG, Brazil

[b] Núcleo de Espectroscopia e Estrutura Molecular, Departamento de Química, Universidade Federal de Juiz de Fora, Juiz de Fora – MG, 36036-900, Brazil

Abstract

Two new 2-naphthyl squaramides, 3-methoxy -4-(2-naphtalenylamino)-3-cyclobutene-1,2-dione (**SQ-NPh1**) and bis-3,4-(2-naphtalenylamino)-3-cyclobutene-1,2-dione (**SQ-NPh2**) were synthesized via condensation reaction between the dimethylsquarate and 2-naphthylamine. The spectrometric characterization by ^{13}C-NMR confirmed the obtaining of the squaramide derivative and nor the squaraine analog. This hypothesis was corroborated by Raman and Infrared spectroscopy since the characteristic vibrational bands related to the oxocarbon portion of both structures have been assigned, such as the ones for **SQ-NPh1** and **SQ-NPh2**. The single-crystal X-ray crystallography for **SQ-NPh1** crystal structures have been solved and the structure of **SQ-NPh2** have been refined using Powder Diffraction state-of-art. The **SQ-NPh1** crystallizes in monoclinic system in P2/c space group. Both squaramides present absorption in the ultra-visible (220-370 nm) and fluorescent emission in the near-infrared (780-800 nm), besides they also presented high thermal stability (around 570 ^{o}C). Generally, only squaraines are reported as NIR emitters, this is the first description of NIR emission for squaramides, and since the synthesis of squaramides is very easy and the rational design of small-molecule NIR fluorophores is of high priority and great value, these results are very promising for the development of novel NIR fluorescent dyes.

Keywords: Squaramides; vibrational spectroscopy, X-ray crystallography, NIR emitters

1. Introduction

Near-infrared (NIR) light is an electromagnetic radiation with a longer wavelength than visible light (400–700 nm), extending from the nominal red edge of the visible spectrum at 700–2500 nm. Near-infrared materials can be classified into two groups: inorganic materials including metal oxides and semiconductor nanocrystals; and organic materials including metal complexes, ionic dyes, extended p-conjugated chromophores [1–3].

NIR-emissive organic materials, or near infrared fluorescence (NIRF) materials, are relatively less available than NIR-absorbing, organic materials [3,4]. As a matter of fact, NIR emitting materials have attracted great attention for potential applications, such as in organic light emitting diodes (OLEDs) [3,5,6], light emitting electrochemical cells [1,7,8], photovoltaic cells [9], chemical sensors [10,11], telecommunications [2] and in night-vision target identification [2,5,12]. It is remarkable that NIR emissive organic materials offer advantages in biological optical imaging, because of no or low NIR auto fluorescence from tissue and deeper penetration of light into the tissues at wavelengths between 650 and 900 nm [1,3,4,13,14].

Some approaches have been established to design NIR-emitting molecules [2,5,6] such as: the introduction of specific substituents, heteroatoms or heterocycles, π-conjugation length [15–20] and donor-acceptor (**D**-**A**) system [1,21–27]. Among many kinds of possible molecular structures, squaraine dyes can be considered a very suitable building block for donor-acceptor type organic dye molecules with intense absorption in the visible to the near infrared region [28]. Squaraine dyes, or 1,3-squaraines, are the condensation products of electron-rich aromatic and heterocyclic molecules such as N,N-dialkylanilines, benzothiazoles, phenols, azulenes and pyrroles with 3,4-dihydroxy-3-cyclobutene-1,2-dione ("squaric acid") [29]. The squaric acid (H2Sq) - 3,4-dihydroxycyclobut-3-ene-1,2-dione or diketocyclobutenediol (**1**) - is a versatile organic building block that can be used in a variety of fields in organic and inorganic chemistry ranging from dyes, optoelectronic materials to bioconjugates due to its interesting structural features such as flat cyclic structures, high molecular symmetry (Dnh), extensive π electron delocalization and these characteristics are similar for their derivatives [30–34]. The condensation between squaric derivatives (squaric acid, the corresponding alkoxy squarates or 3,4- squarate dichloride, electron-acceptor unit, **A**) and aromatic amines (electron-donating unit, **D**) can yield the donator-acceptor systems 1,3-squaraine (**2**) or 1,2-squaramide (**3**) adducts [30,31,34,35]. The partial or total substitution of the oxygen atoms in the squaric acid (H_2Sq) by amino groups engenders the so-called mono- (**3a**) and di-substituted (**3b**) squaramides, and the most notable body of work has been around the development and application of these nitrogenous derivatives [31,34]. The squaramides and other derivatives can be generally prepared by condensation of electron-rich aromatic, heteroaromatic or olefinic compounds with squaric acid [30] or with dialkoxysquarate derivatives (named diethersquarates or diestersquarates **4**, the most widely used substrates for their synthesis [31,32,36]. Squaramides have been known to possess remarkable

ring systems, structural rigidity, and high affinity for hydrogen bonding, and to provide some interesting chemical and physical applications [37–39] because their species show strong absorption bands in the visible region, intense fluorescence emission [40] and good photoconductivity [41,42]. The useful and unique absorption and fluorescence properties of squaraines are remarkable for a variety of applications and the possible control of the properties by electron-acceptor or electron-donating units can lead to absorption at lower energy and in the red to NIR regions which is important and promising for dye-sensitized and organic photovoltaic cells [28,43,44]. It has been recognized that for conventional squaraines the fluorescence might be easily shifted deep into the NIR region through the addition of dicyanovinyl groups into the framework, and this strategy also enhances NIR fluorescence properties and chemical robustness [45–48].

As cited before, the introduction of specific substituent groups electron donor-acceptor (**D**-**A**) system is a well-established methodology to design NIR-emitting molecules [1,21–27] and molecular hybrid squaraines, or 1,2-squaramides whit donor-acceptor systems (**D**-**A**) can be made connecting the squaric electron-acceptor unit (**A**) and electron-donating substituents (**D**) through the chemical reaction between high reactive electrophilic squaric derivatives and fluorescent aromatic amines. The investigation of the synthesis of new amino-squaric (squaraine or squaramide) derivatives obtained with electron-donor and fluorescent substituents in order to achieve novel NIR molecular emitters is very promising.

Herein, we report the synthesis and the NIR emission investigation of two new 1,2-squaramides with donor-acceptor (**D**-**A**) molecular hybrid system: 3-methoxy-4-(2-naphtalenylamino)-3-cyclobutene-1,2-dione (**SQ-NPh1**) and bis-3,4-(2-naphtalenylamino)-3-cyclobutene-1,2-dione (**SQ-NPh2**) obtained through direct condensation reactions between 2-aminenaphtalene (**5**) and 3,4-dimethoxy-3-cyclobutene-1,2-dione (**4**).

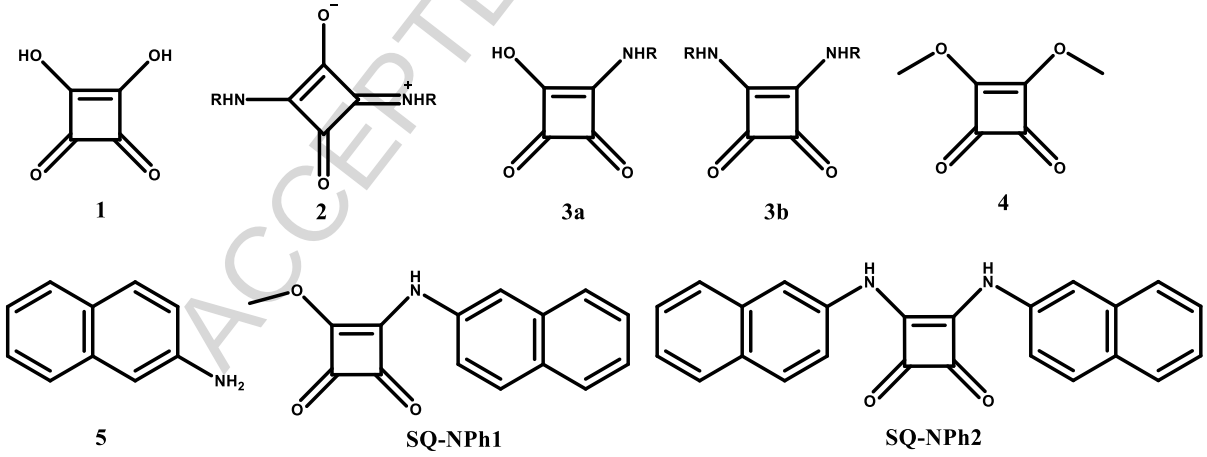

Figure 1. Squaric derivatives, the precursor molecules and the novel squaramides investigated

2. Experimental

2.1. Chemicals and Reagents

Squaric acid (H_2Sq) was purchased from Sigma-Aldrich, 2-aminenaphthyl was obtained from Combi-Blocks and both were used as received without further purification.

2.2. Synthesis

*2.2.1. Obtaining of 3,4-Dimethoxy-3-cyclobutene-1,2-dione (**4**)*

A solution of 0.30 g (2.6 mmol) of squaric acid (**1**) and 0.80 g (4.1 mmol) of concentrated sulfuric acid in 25 mL of anhydrous methanol in a round-bottomed flask equipped with a reflux condenser was heated until reflux for 24 hours. After the reaction was complete, the solution was cooled, neutralized with saturated sodium bicarbonate solution and extracted with 3 x 50 mL of dichloromethane. The organic phase was then dried with anhydrous magnesium sulfate, filtered and evaporated to afford 0.32 g (87 %) of a yellow oil. IR (ATR, cm^{-1}): 2996 ($\nu_{c\text{-}H}$), 1809 ($\nu_{C=O}$), 1638 ($\nu_{C=C}$), 1266 ($\nu_{C\text{-}O}$), 735 ($\delta_{C\text{-}H}$). ^{1}H NMR (400 MHz, $CDCl_3$-d^1) δ 4.37. ^{13}C NMR (400 MHz, $CDCl_3$-d^1) δ 61.22, 184.67, 189.39.

*2.2.2. Preparation of 3-Methoxy -4-(2-naphthalenylamino)-3-cyclobutene-1,2-dione (**SQ-NPh1**)*

A solution of 0.10 g (0.70 mmol) of 2-aminenaphthyl (**5**) in 15 mL of methanol was added to a homogeneous solution of dimethylsquarate (**2**) (0.10 g, 0.7 mmol) and methanol in a 25 mL round bottom flask equipped with a magnetic stirrer and a reflux condenser. The mixture was stirred for 12 hours at room temperature and a solid was obtained. The obtained yellowish solid was recrystallized with tetrahydrofuran (65%). MP: 219,5 -220,0 °C. IV (ATR, cm^{-1}): 3261 ($\nu_{N\text{-}H}$), 1802 ($\nu_{C=O}$), 1709 ($\nu_{C=O}$), 1639 ($\delta_{C\text{-}N\text{-}H}$), 1595 ($\delta_{N\text{-}H}$), 1398($\nu_{C=C}$), 1260 ($\nu_{C\text{-}N}$). ^{1}HNMR (400 MHz, DMSO-d^6) δ 4.40 (3H); 7.42 (1H, *t*,*J*=7.5); 7.49 (1H, *t*, *J*=7.2); 7.55 (1H, *d*,*J*= 8.76); 7.79-7.81 (2H, m); 7.86 (1H, *d*,*J*=8.05,); 7.90 (1H, *d*, *J*=8.94) 10.95 (1H). ^{13}C NMR (400 MHz, DMSO-d^6) δ60.59, 115.84, 119.85, 125.08, 126.81, 127.25, 127.60, 128.88, 129.97, 133.19, 135.60, 169.25, 178.92, 184.02, 188.07. ESI-MS *m/z* $[SQ\text{-}NPh1+Na]^+$: Calculated for $C_{15}H_{11}NO_3$: 276.0636, Found: 276.0631.

*2.2.3. Preparation of bis-3,4-(2-Naphthalenylamino)-3-cyclobutene-1,2-dione (**SQ-NPh2**)*

To a magnetically stirred mixture of dimethylsquarate **4** (0.10 g, 0.70 mmol) and methanol was added 2-aminenaphtalene **5** (0.20 g, 1.4 mmol) dissolved in 25 mL of methanol. The mixture was stirred during 24 hours

at room temperature. The solid obtained was filtered and purified by recrystallization from dimethylsulfoxide to yield a yellow crystalline product (56%).MP > 300 °C. IV (ATR, cm^{-1}): 1785 ($\nu_{C=O}$), 1667 ($\nu_{C=O}$), 1632 (δ_{C-N-H}), 1587 (δ_{N-H}), 1381($\nu_{C=C}$), 1270 (ν_{C-N}).);^{1}H NMR (400 MHz, DMSO-d6) δ 7.42 (2H, *t*, *J*= 7.7); 7.50 (2H, *t*, *J*=7.3); 7.69 (2H, *d*, *J*= 8.8); 7.82-7.88 (4H); 7.94-7.96 (4H); 10.14 (2H).^{13}C RMN (400 MHz, DMSO-d^6) δ114.54, 119.24, 124.85, 126.90, 127.17, 127.67, 129.29, 129.66, 133.52, 136.25, 165.87, 181.94.

2.3. Instrumentation

Melting points were determined on a Micro-Química apparatus MQAOF-301. The characterization of compounds was performed by vibrational spectroscopy (Raman and infrared). Raman spectra were collected from solid phase using a Bruker RFS 100 FT-Raman instrument equipped with Ge detector refrigerated by liquid nitrogen, with excitation at 1064 nm from a Nd:YAG laser, power of 100 mWat the sample, in the range between 3500 and 100 cm^{-1}, and spectral resolution of 4 cm^{-1}, with an average of 512 scans. Diffused reflectance infrared Fourier Transform (DRIFT) spectra were recorded in an Alpha Bruker FT-IR spectrometer, in the region 4000-400 cm^{-1}, with 4 cm^{-1} of spectral resolution, and average of 128 scans. The background spectrum was recorded with the DRIFT cell filled with KBr and the sample spectrum was diluted in KBr.^{1}H and ^{13}C NMR spectrometry were performed at 400 MHz on a Brüker DPX 400 advance spectrometer, using solvents as internal references. Chemical shifts (δ) are reported in parts per million downfield from tetramethylsilane (TMS) and in DMSO-d^6. Thermogravimetric analysis (TGA) was performed by TA Instruments TGA Q5000 under a dry nitrogen gas flow at a heatingrate of 5 °C/min. Ultraviolet–visible (UV–vis) absorption spectra were recorded using a Shimadzu UV-2550 UV/VIS spectrometer. The PL spectra were recorded using a Cary Eclipse Fluorescence Spectrophotometer (Xe pulse lamp, pulsed at 80 Hz). High resolution electrospray ionization mass spectra were included in the Bruker Micro TOF - Q II spectrometer. The measurements of X-ray diffraction by single crystal for **SQ-NPh1** were carried out in a diffractometer Supernova Agilent with CCD area detector ATLAS S2, using MoKα radiation (α = 0.71073 Å) at room temperature. The data collection, reduction, unit cell refinement and absorption correction were performed using Crysalis RED software (Oxford Diffraction Ltda, version 171.39.46) [49]. The structures were solved and refined using crystallography programs SHELX-2018/3 [50]. The structures were drawn using the programs ORTEP-3 for Windows [51] and mercury [52]. The diffraction data for bis-3,4-(2-naphtalenylamino)-3-cyclobutene-1,2-dione (**SQ-NPh2**) were collected by overnight scans in the 2θ range of 4-105° with step of 0.02° using a *Bruker AXS D8 Da Vinci* diffractometer, equipped with Ni-filtered CuKα radiation (λ=1.5418 Å), a Lynxeye linear position-sensitive detector was used and the following optics were set up: primary beam Soller slits (2.94°), fixed divergence slit (0.3°) and receiving slit 7.68 mm. The generator was set up at 40 kV and 40 mA. Approximate unit cell parameters were determined using about 21 low-angle peaks, followed by indexing through the single-value decomposition approach [53] implemented in TOPAS [54]. Interesting point out that

the space group $P2_1/c$ gave the same R_{pw} that space group $P_{2/c}$. However, the peak 010 at 14.3 (2theta), which has very low intensity, is present and the space groups P_2/c was chosen for **SQ-NPh2** and cell parameters were eventually refined using diffraction data up to 55° (2θ) range by the Pawley method [55]. In the present case no higher symmetry transformations were suggested by PLATON [56]. The structure solution process was performed by the simulated annealing technique [57] also implemented in TOPAS, where only a half **SQ-NPh2** molecule has been drawing by Z-matrix formalism. The translation of half **SQ-NPh2** molecule, located at the center of the square moiety, has been fixed at special position 0.5x 0.5y 0.75z, as similar other structures solved by powder diffraction data studies [58–60]. In simulated annealing step, rotation and two torsion angles of **SQ-NPh2** were left free. In the final refinement stage, carried out by the Rietveld method [61], 37 parameters were refined, including 12 coefficients for the background contribution modeled by a Chebyshev polynomial function. An overall isotropic thermal parameter model 0.3(3) was employed for all atoms. The final Rietveld refinement plot is described as supplementary information – Figure S12.

Cambridge Crystallographic Data Centre (CCDC) - 1897505 contains the supplementary crystallographic data for **SQ-NPh1.** Crystal data, fractional atomic coordinates and displacement parameters of seven crystal structure described for **SQ-NPh2** are supplied in standard CIF deposited in the CCDC under number 1894166. These data can be obtained free of charge via https://www.ccdc.cam.ac.uk/structures/, or by e-mailing data_request@ccdc.cam.ac.uk, or by contacting The Cambridge Crystallographic Data Centre, 12 Union Road, Cambridge CB2 1EZ, UK; fax: +44(0)1223-336033.

3. Results and Discussion

3.1. Synthesis of the investigated 2-naphthyl squaramides **SQ-NPh1** and **SQ-NPh2**

The mono- and disubstituted squaric derivatives **SQ-NPh1** and **SQ-NPh2** were synthesized in an efficient two-step straight forward route as reported in Figure 1. The dimethylsquarate **2** was obtained in good yield (87%) by direct condensation of squaric acid (**1**) with concentrated sulfuric acid and methanol in excess. Other attempts to prepare this starting material were tried, but none of them were so easy and efficient [62,63]. The synthesis of these novel compounds, in reasonable yields, were carried out from the condensation reactions at room temperature between dimethylsquarate **4** and 2-naphthylamine **5**: mono-naphthyl analog **SQ-NPh1** was obtained with the amine in equimolar amounts (Fig. 2) and the corresponding disubstituted **SQ-NPh2** was prepared with bis-equimolar amount of the amine and longer reaction. In fact, it has been related that the synthesis of mono-amino-squaraines could be achieved through direct reaction of squaric acid (**1**) with amines in methanol, and that in DMF the 1,3-diaminosquaraines would be obtained as major product and the corresponding mono- and di-squaramides as minor products [35,64,65]. The mono-squaramide would be preferentially obtained in water, with or without acid catalysis [66], and the microwave-assisted preparation in

water gives selectivity for the mono-squaramide [64]. The dichloride squarate was also prepared [67], but the subsequent reaction with 2-naphthylamine [67,68] did not yield the products with easiness for purification. It has been cited [32], that squaric acid diesters can effectively be used as starting materials to 1,3-squaramides synthesis, and they are able to couple two different amino-functionalized molecules for the preparation of non-symmetrical bis-squaramides. The obtained results herein confirm that in order to synthesize the corresponding mono- or bis-squaramides with selectivity, the utilization of methanol as solvent is a suitable methodology, in accordance with the literature [31,64].

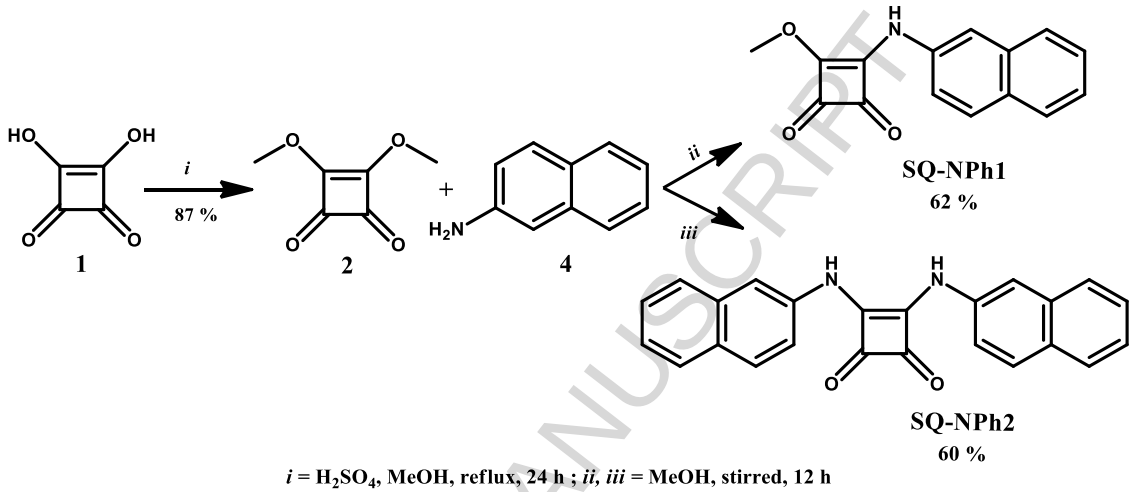

Fig. 2. Synthetic route for obtaining of SQ-NPh1 and SQ-NPh2

The analysis of the IR and Raman spectra (Table 1, Figures 3 and 4) of **SQ-NPh1** and **SQ-NPh2** revealed that both compounds present characteristic carbonyl vibration bands from squaramide structure, respectively at 1802, 1709 cm^{-1} and 1785, 1667 cm^{-1}. Some important bands can be assigned to the oxocarbon portion of both structures, such as the ones at 1805 cm^{-1} for **SQ-NPh1** and at 1788 $cm^{-1}$for **SQ-NPh2** in the Raman spectra, which are assigned to the CO stretching mode; the same vibrational mode can be seen at 1802 $cm^{-1}$and 1785 cm^{-1}, respectively, in the infrared spectra. The C=O stretching vibration coupled with C=C stretching mode can be assigned to the band at 1714 cm^{-1} (1709 cm^{-1} in the infrared) for the **SQ-NPh1** and at 1662 cm^{-1} (1667 cm^{-1} in the infrared) for **SQ-NPh2**. The ring breathing mode can only be observed in the infrared spectrum at 729 cm^{-1} for **SQ-NPh2**, whereas the ring angular deformation shows up at 615 cm^{-1} (614 cm^{-1}in the IR) for mono-derivative and at 592 cm^{-1} (586 cm^{-1} IR) for bis-derivative. Bands observed at 3060 cm^{-1} in the Raman spectra are assigned to the 2-aminonaphthyl ring portion, and can be also observed at 3057 cm^{-1} in the infrared spectra (for mono-analogue, **SQ-NPh1**) and 3054 cm^{-1} (bis-, **SQ-NPh2**). Other vibrational modes, such as the angular deformation and amine stretching, can be assigned to the bands at 1642 and 1264 cm^{-1}, respectively in the Raman spectra for **SQ-NPh1**, and at 1636 cm^{-1} and 1270 $cm^{-1}$for **SQ-NPh2**. The very characteristic naphthyl amine band is assigned to the Raman peak at 1398 cm^{-1} for mono-substituted and 1385 cm^{-1} for bis-substituted analogue, whereas the ring breathing mode for the mono-substituted can be seen at 754

cm^{-1} (753 cm^{-1} IR) and for bis-substituted at 756 cm^{-1} (751 cm^{-1} IR). The COC stretching mode can be seen at 1037 cm^{-1} for **SQ-NPh1** in the Raman spectrum, and this band can be used for the differentiation between the two structures, since the **SQ-NPh2** does not present this molecular group. It is worth of mention the band at 467 cm^{-1}, assigned to the NH angular deformation for mono-substituted compound and at 478 cm^{-1} for bis-substituted.

Table 1
Suggested vibrational assignment of **SQ-NPh1** and **SQ-NPh2** all values are given in wavenumbers (cm^{-1})

SQ-NPh1		SQ-NPh2		Tentative
Raman	**IV**	**Raman**	**IV**	**Assignment**
3260	3261	n.d.	n.d.	ν_s(NH)
3060 (w)	3057 (w)	3060 (w)	3054 (w)	ν(CH) of 2-NFT ring
1805 (w)	1802 (m)	1788 (w)	1785 (m)	ν(CO) squarate ring
1714 (w)	1709 (s)	1662 (w)	1667 (s)	ν(CO) + ν(CC) squarate ring
1642 (s)	1639 (w)	1636 (s)	1632 (w)	δ(CNH)
1590 (w)	1595 (s)	1587(w)	1587 (m)	δ(NH) + ν(CC) 2-NFT ring
1478 (m)	1472 (w)	1470(m)		δ(CH)
1398 (s)	1398 (w)	1385(s)	1381 (w)	ν(CC) of 2-NFT ring
1264 (w)	1260 (w)	1270(m)	1270 (m)	ν(CN)
1230 (w)	1228 (w)	1226(m)	1225 (w)	δ(CH) + ν(CC) of 2-NFT ring
1197 (w)	1192 (w)	1196 (m)	n.d.	ν(CN) + δ(CH) + ν(CC) of 2-NFT ring
1097 (w)	1094 (w)	1088 (w)	1088 (w)	ν(CC) squarate ring
1037 (w)	1037 (w)	n.d.	n.d.	ν(COC)
779 (m)	774 (w)	777 (m)	777 (w)	δ(CCC)
754 (m)	753 (m)	756 (w)	751 (w)	2-NFT ring breath
n.d.	n.d.	729	n.d.	Squarate ring breath
615 (w)	614 (w)	592 (w)	586 (m)	δ (squaratering)
n.d.	467	n.d.	478	δ(NH)

ν_s, symmetrical; ν,stretching; δ, angular deformation; n.d.= non-detected stretching

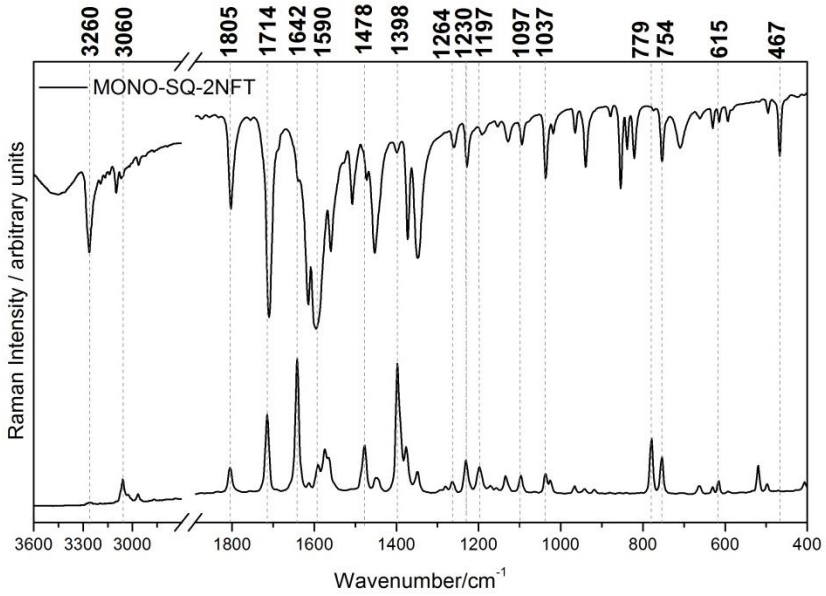

Fig. 3. Infrared and Raman spectra (1064 nm) of **SQ-NPH1**

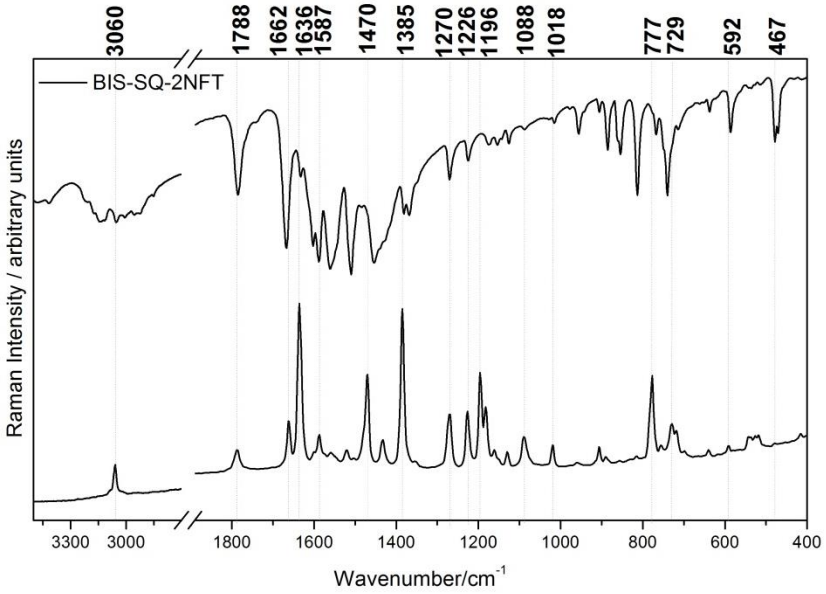

Fig. 4. Infrared and Raman spectra (1064 nm) of **SQ-NPH2**

The ^{13}C-NMR spectra analysis corroborated the mono-squaramide structure obtaining for **SQ-NPh1,** since two signals corresponding to different carbonylic carbons were assigned (δ 188.07 and 184.02 ppm) and none detection of signals related to squaraine carbons, usually appearing around δ 175 ppm [64,69]. **SQ-NPh2** also presented in its ^{13}C-NMR spectrum only one carbonyl carbon signal (δ 181.94 ppm) as expected for a symmetrical 1,2-bis-squaramide. It is noteworthy, as previously cited, that generally according to the literature the reactions with aromatic amines can also give the 1,3-squaraines, alongside the desired 1,2-squaramides adducts [34-41], however in the cases reported herein, only the corresponding 3-methoxy-4-aminonaphthyl-**SQ-NPh1** and bis-3,4-bis-naphthyl-squaramides **SQ-NPh2** were obtained.

*3.2. Crystal Structure of mono-2-naphthyl squaramide (**SQ-NPh1**) and bis-2-naphthyl squaramide (**SQ-NPh2**)*

The structures of squaramides **SQ-NPh1** and **SQ-NPh2** were elucidated by single and powder X-ray diffraction, respectively. The crystal data for both compounds are displayed in Table 2.

Table 2
Crystal data for compounds **SQ-NPh1** and **SQNPh2.**

Compound	**SQ-NPh1**	**SQ-NPh2**
Formula	$C_{15}H_{11}NO_3$	$C_{24}H_{16}N_2O_2$
Molecular mass / g mol^{-1}	253.25	364.40
Crystal System	Monoclinic	Monoclinic
Space group	$P2_1/n$	P2/c
a / Å	7.4310(4)	17.479(4)
b / Å	7.6077(3)	6.155(3)
c / Å	21.316(1)	8.031(3)
α / °	90.000	90.00
β / °	92.392(5)	93.18(4)
γ / °	90.00	90.00
V / Å^3	1204.0(1)	862.84(5)
Temperature / K	293(2)	293(2)
Z	4	2
D_{calc} / g cm^{-3}	1.397	1.4026(9)
Crystal size / mm	0.15 x 0.37 x 0.91	-
μ(Mo Kα) / cm^{-1}	0.098	-
μ(Cu Kα) / mm^{-1}	-	72.64(5)
Measured / independent reflections	15485 / 3125	-
R_{int}	0.0431	-
Observed reflections [$F_o^2>2\sigma(F_o^2)$]	2428	-
Parameters	172	37
$R_{Bragg;}$ R_{wp}	-	0.032; 0.187
R_{obs} [$F_o>2\sigma(F_o)$]	0.0590	-
R_{all}	0.0744	-
wR_{obs} [$F_o^2>2\sigma(F_o)^2$]	0.1725	-
wR_{all}	0.1870	-
S	1.069	-
RMS / e Å^{-3}	0.052	-

*3.2.1. X-ray crystallographic results of mono-2-naphthyl squaramide **SQ-NPh1***

The single-crystal x-ray data confirm that the compound **SQ-NPh1** is a mono-substituted compound, as can be seen in Figure 5. Selected geometrical parameters for this compound are displayed in Table 3.

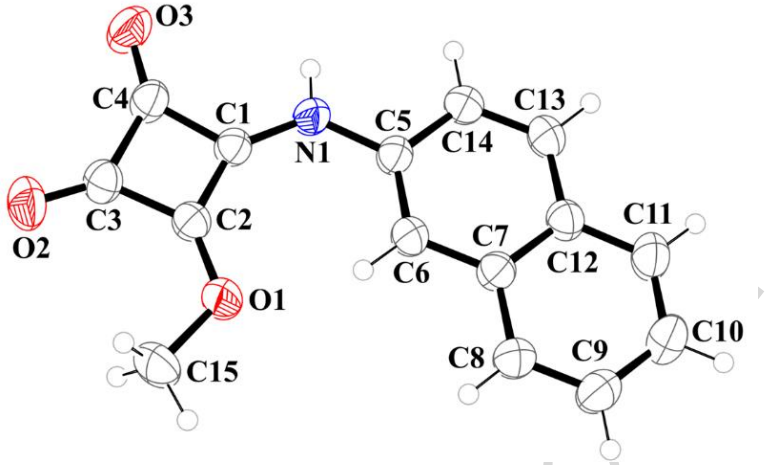

Fig. 5. Ortep representation of squaramide **SQ-NPh1**. The displacement ellipsoids were drawn at 50 % probability level.

The molecule of **SQ-NPh1** is almost planar presenting an average deviation of the best plane equal to 0.023 Å and the angle between ring planes (squaramide ring and naphthyl ring) of 1.17(9)°. The biggest deviation of molecular plane was observed for atom O3 (0.060(2)Å). As observed elsewhere and in the structure of **SQ-NPh1** (Figure 4) herein there are well-known similarities between amides and squaramides, but additionally the squaramide presents the rigid and planar structure of the cyclobutadienedione ring containing two coplanar carbonyls and two NHs that are almost coplanar. This arrangement is stabilised by the nitrogens that are essentially sp2-hybridised, making the lone pairs available for conjugation from N(p-orbital) into the p-system orthogonal to the plane. The mutual influence of a squaramide NH and a carbonyl oxygen on the overall structure is reflected as a partial contribution of limiting zwitterionic structures that restricts the rotation around the C–N bonds of squaramides [70]. In **SQ-NPh1** the distance of N1 to squaramide plane is 0.014(3) Å indicating the coplanarity of this squaramide, as expected.

The average of C-C bond in squaramide ring is 1.462(2) Å and the higher CC bond length difference (ΔCC) is 0.118 Å. These values for sodium squarate salt are 1.4707(8) and 0.0247 Å [71] and 1.461(2) and 0.067 Å for 1,2-dianilinosquairane [31,72]. The CC length is very similar for these compounds, however the ΔCC is smaller for sodium squarate and 1,2-dianilinosquairane, suggesting that the electronic delocalization in **SQ-NPh1** is less effective. However, a more detailed observation of the 3D packing arrangement (Figure 5a) shows the existence of interactions between the squaramide and the naphthyl rings suggesting the π-stacking interactions, in analogy to another work with bis-2-pyridylethylamine-squaramide [31,73]. The topological analysis [74] of this interaction in **SQ-NPh1** shows that presence of two different π-stacking among sqluaramide and naphthyl rings. The centroid-centroid distances are 3.44 and 3.59 Å, the interplanar distances

are 3.42 and 3.50 Å, presenting short shifts between the rings (0.39 and 0.79Å). These analyses confirm that the π-stacking is present in this structure and is important for crystal packing stabilization. These interactions form a 1D arrangement along of ***a*** crystallographic axis. In this compound was verified the presence of a medium intermolecular hydrogen bond formed by NH and O atom of squaramide ring (N···O distance of 2.935(2) Å) forming a dimeric structure (Figure 5b). The association of the NH···O and π-stacking interations gives rise a two dimensional arrangement in solid state as can be seen in Figure 5c.

Table 3
Selected bond distances and angles for **SQ-NPh1**.

Bond distance / Å			
C2-O1	1.313(2)	C5-N1	1.413(2)
C15-O1	1.451(2)	C1-C2	1.394(2)
C3-O2	1.209(2)	C1-C4	1.466(2)
C4-O3	1.208(2)	C2-C3	1.475(2)
C1-N1	1.341(2)	C3-C4	1.512(3)
Bond angle / °			
C1-C2-O1	132.1(2)	C4-C1-N1	127.0(2)
C3-C2-O1	134.7(2)	C2-C1-N1	141.7(2)
C2-C3-O2	137.2(2)	C1-N1-C5	130.3(2)
C4-C3-O2	136.3(2)	C6-C5-N1	123.7(2)
C3-C4-O3	137.3(2)	C14-C5-N1	116.2(2)
C1-C4-O3	133.8(2)		

Additionally, in **SQ-NPh1** was observed the **CH···O** hydrogen bond interactions in the crystal structure stabilization. The interactions among CH of methyl group and O2 atoms form a chain along ***b*** axis (Figure 6). Similar interactions were also observed among CH of naphthyl and O3 atoms giving rise to a dimer, which in association with $CH_{(methyl)}$···O form a bi-dimensional (2D) arrangement (Figure 7). The geometrical parameters of hydrogen bonds are listed in Table 4.

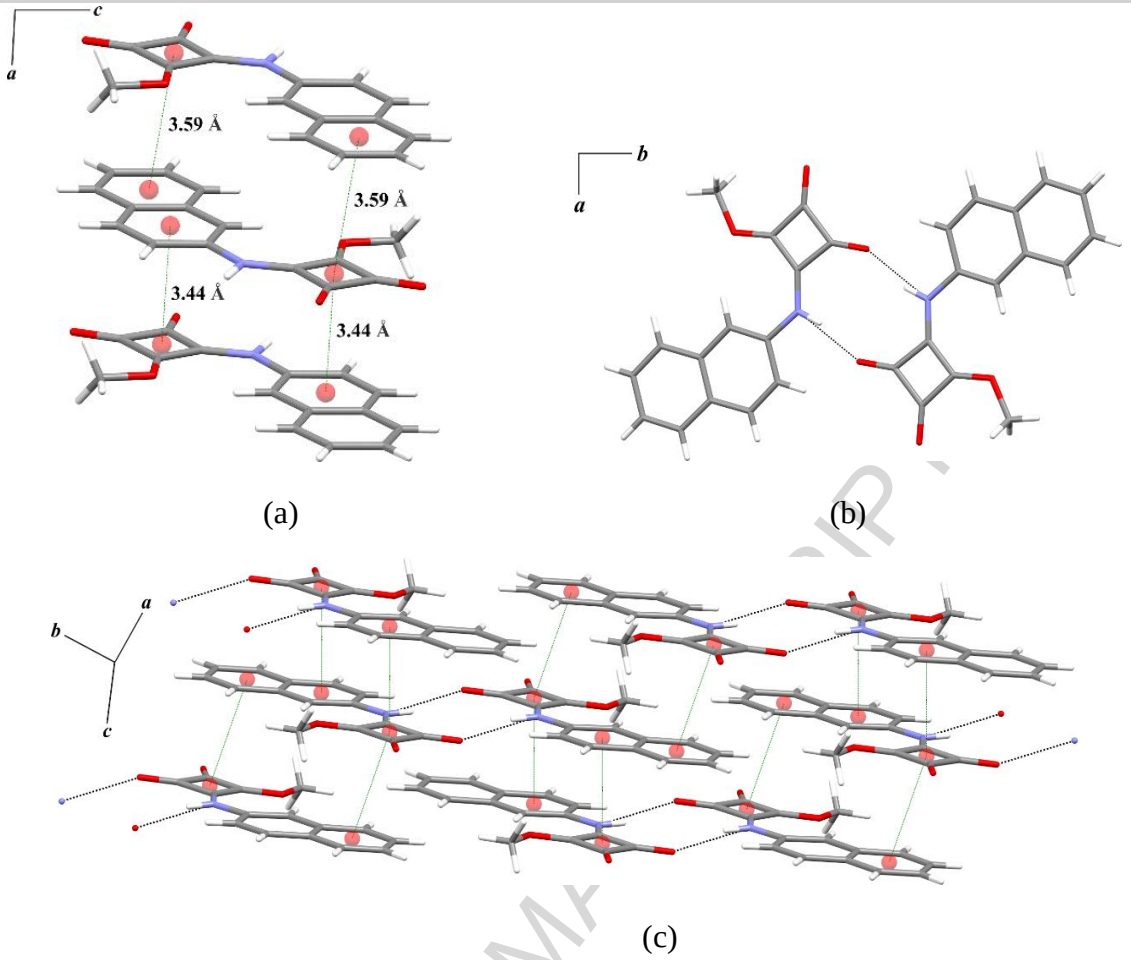

Fig. 6. The intermolecular interactions in **SQ-NPh1**: a) π-stacking, b) NH···O hydrogen bonds and c) 2D arrangement.

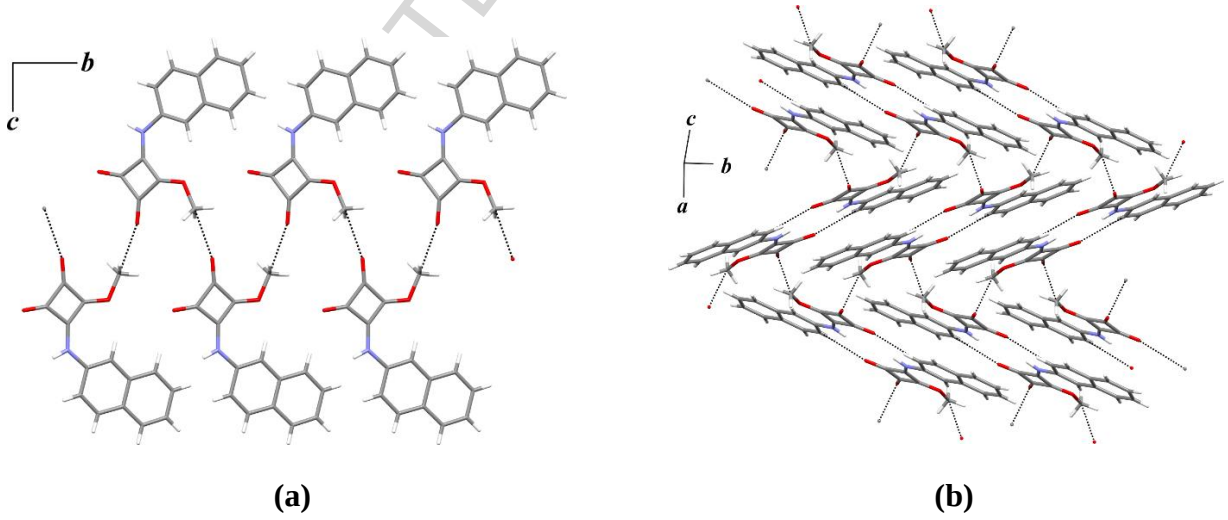

Fig. 7. CH···O hydrogen bond interactions in **SQ-NPh1** view along ***a*** axis: a) $CH_{(methyl)}$ ···O and b) $CH_{(methyl)}$ ···O and $CH_{(naphthyl)}$ ···O.

Table 4

Hydrogen bond geometry in **SQ-NPh1.**

D-H···A	D-H / Å	H···A / Å	D···A / Å	D-H···A / °
N1-Hn···O3^{i}	0.85	2.110	2.935(2)	164
C15-H15b-O2^{ii}	0.96	2.642	3.098(3)	109
C14-H14-O3^{i}	0.93	2.526	3.277(3)	138

Symmetry code: *i* (1 - *x*, -1 - *y*, - *z*), *ii* (½ - *x*, ½ + *y*, ½ - *z*)

Since it can be assumed the restricted rotation about the C-N of squaramides, it might exist different conformational arrangements between the C-N(-H)(-Ar) and the C-(O)-(Me) groups, they can be in *syn*/*anti* conformations. In Figure 4 it can be seen that the molecule has the methoxyl group in opposite side to the N-H amide bond, and the ether oxygen atom is directed to the *alpha*-H from the naphthyl groups, like an unusual *syn/syn* conformation that is not commom in bis-squaramides [31] that normally prefer the *anti/anti* or *syn/anti* conformations in order to favour inter- or intra- hydrogen bonds [31,38,75,76]

*3.2.2. Crystal Structure discussion of bis-2-naphthyl squaramide **SQ-NPh2***

In absence of suitable single crystal of **SQ-NPh2** its crystal structure model was achieved using powder diffraction *state-of-the-art* data measured on conventional laboratory equipment. The crystallographic parameters of **SQ-NPh2** were summarized in Table 5 while selected bond distances are given in Tables 2 and 6**.** The molecular structures of **SQ-NPh2**, drawn using SCHAKAL [77], is depicted in Fig. 8. It's worth pointing out that the **SQ-NPh2** molecule is not planar, in solid state, the angle formed between naphthyl rings is about 50^{o}. In the Fig. 9 the hydrogen bonds along *b* axis were depicted. As expected, the hydrogen bonds were located between NH and O=C groups, where the distance NH...OC is about 1.946Å and in a *anti/anti* conformation, as usually observed for bis-squaramides [31]. This result is also in according to the data obtained for dibenzyl squaramide investigated by Puigjaner, Prohens et. al [31,76] that remarks the presence of cooperative H-bonding between monomers.

Table 6
Main angle and length bonds of **SQ-NPh2**.

Lengths / Å		Angle / ^{o}	
C2-O3	1.251(4)	O3-C2-C1	135*
C1-C2	1.490(1)		
C1-C1^{i}	1.486(1)	C2-C1-N1	135*
C2-C2^{i}	1.461(3)		
C1-N1	1.350(1)	C1-N1-C5	125.02(6)
N1-C5	1.489(5)		

*Symmetry codes i 1-x, y,1.5-z * defined in the rigid body*

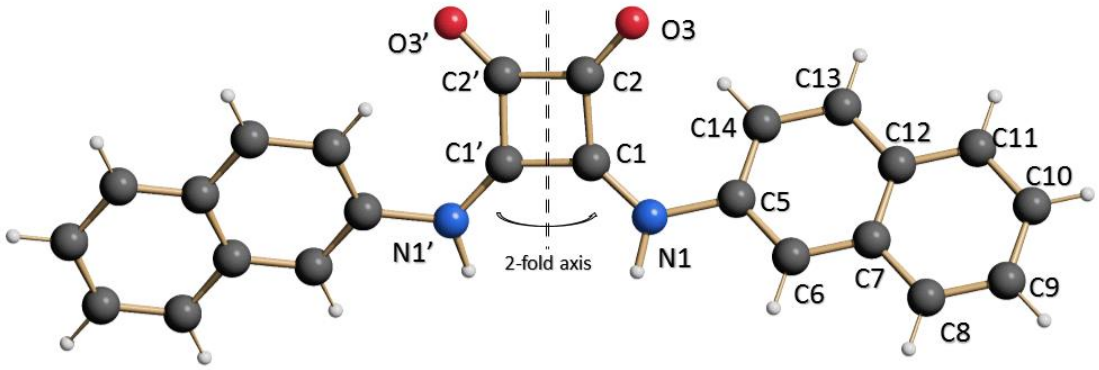

Fig. 8. SCHAKAL plot of **SQ-NPh2** molecule. Carbon, hydrogen, nitrogen and oxygen atoms are colored in dark gray, white, blue and red, respectively.

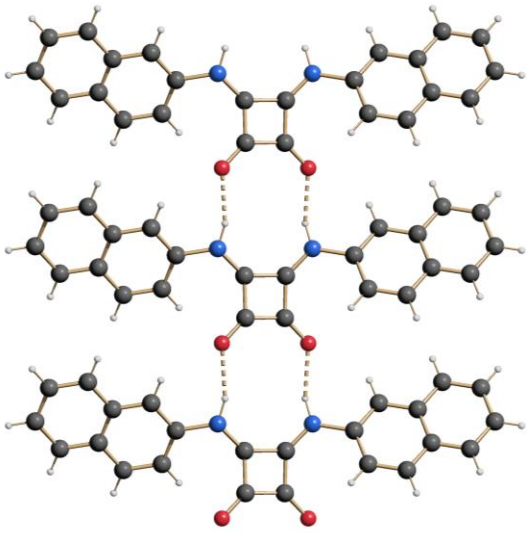

Fig. 9. Intermolecular hydrogen bonds between NH…O=C groups.

3.3. Thermogravimetric analysis

The thermogravimetric analysis was performed for squaramides **SQ-NPh1** and **SQ-NPh2** in nitrogen atmosphere (Figure 10). It can be seen that the TG curves for the mono-squaramide **SQ-NPh1** do not show any weight loss until 265 °C, and at this temperature the fusion process occurs. The bis-squaramide **SQ-NPh2** is stable until 350 °C and for both squaramides above the temperature of 570 ^{o}C occurs the thermal decomposition

in exothermic events. This quite high thermal stability suggests possible applications of these compounds as novel NIR emitters even with incident lasers [69].

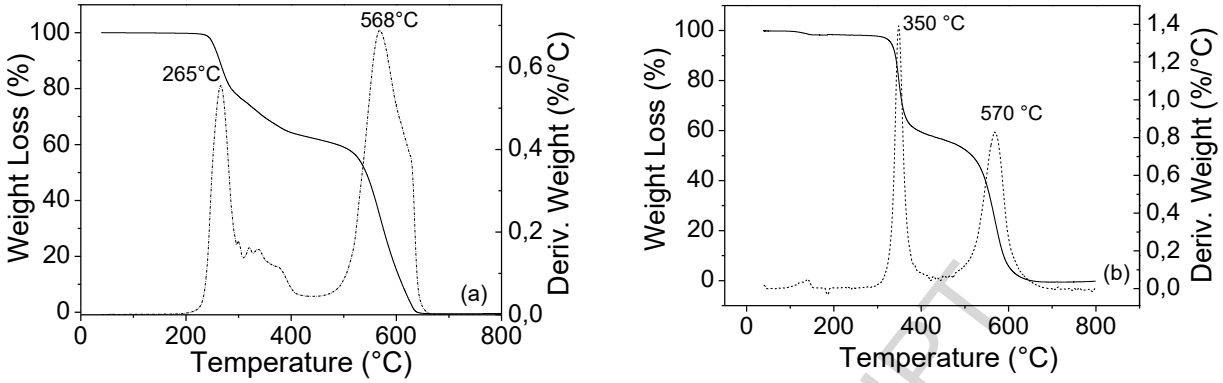

Fig. 10. TG-DTG curves of a) mono-squaramide**SQ-NPh1** and b) bis-squaramide**SQ-NPh1.**

3.4. Electronic Absorption spectra

The UV-visible absorption spectra (Figure 11) for **SQ-NPh1** and **SQ-NPh2** were carried out in DMSO (concentration of 1.10^{-8} M) The observed range of absorption is in quite low energy from 220 to 370 nm and there is no other absorption until 1100 nm. The di-aminonaphthyl squaramide **SQ-NPh2** presents absorption at higher wavelength and consequently lower energy gaps due to the higher conjugation generated by the presence of two aromatic groups.

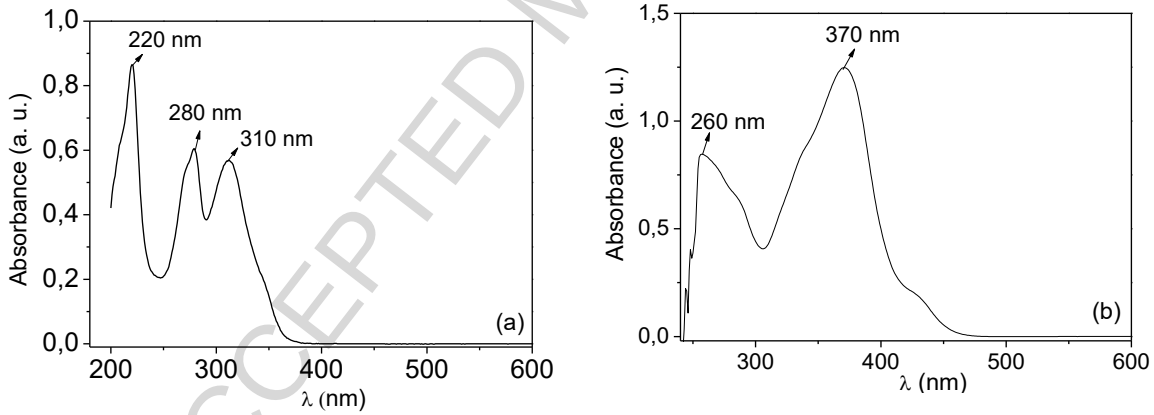

Fig. 11. UV-visible absorption spectra in DMSO of a) mono-squaramide**SQ-NPh1** and b) bis-squaramide**SQ-NPh1**

3.5. Fluorescence Spectroscopy

Fluorescence emission properties of the squaramides were also investigated for **SQ-NPh1** and **SQ-NPh2**, with excitation at 310 and 370 nm respectively, and the fluorescence emission spectra are shown in Figure 12. The stronger emissions were observed in both of them at around in the near-infrared region, respectively at 750 to 780 nm, and in the mono-derivative weaker emissions were detected around 800 to 850

nm. These intense and unique absorptions and fluorescence properties observed for these novel squaramides are worthy requirements for a variety of photochemical applications, such as for dye-sensitized and organic photovoltaic cells among others. It is remarkable, that this is the first description of NIR emission for squaramides, usually only squaraines with a great variety of molecular substitutions are reported as NIR emitters [28,29,45–48].

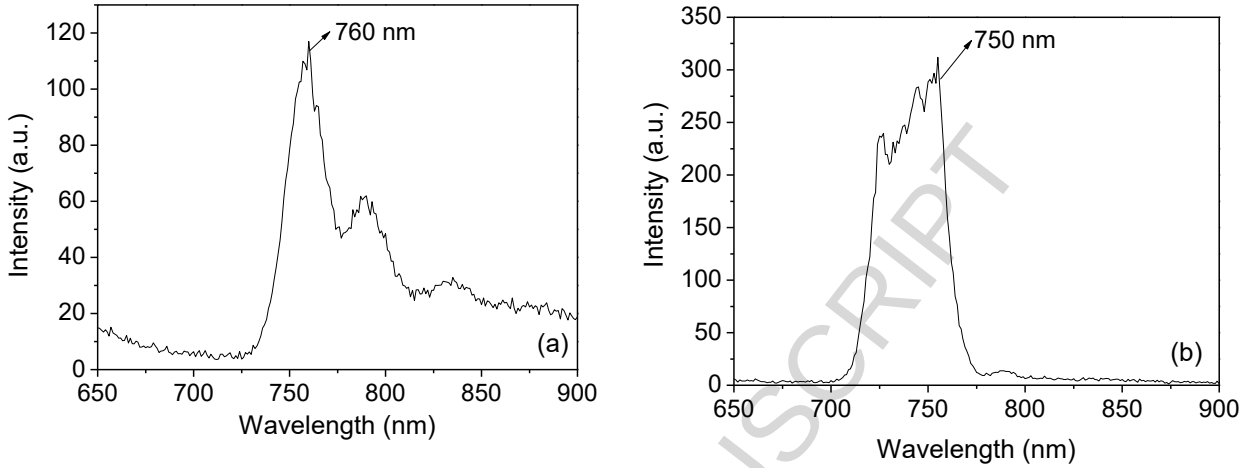

Fig. 12. Fluorescence spectra of a) **SQ-NPh1** and b) **SQ-NPh2** in acetonitrile.

In the literature, there are some noteworthy specific squaraines with intense NIR emission, such as the indolenine squarylium dyes with additional electron-donating amine centers [42] or with emission at 900 nm as the malononitrile-methylquinolinium squaraines [78]. Really, the syntheses of squaraines are a little more complicated [79], especially in some cases as the bis-squaryllium squaraines with thiophene spacers, also with emission at ≅ 800 nm, synthesized by Nakazumi, Yagi and co-workers e Stille-type Pd-catalyzed cross-coupling reaction [80]. However, squaramides are even easier and simpler to be obtained than squaraines, and generally expensive and complicated catalytic methodologies are not needed becoming possible the investigation of a wide variety of novel derivatives even on large scales for industrial application.

3.6. Solvent Effect on Fluorescence Spectroscopy, Solvatochromic effect

It is well-known the effect of the different polarity of the solvents on UV-vis/near-IR absorption spectra [81,82] and even the solvent dependence of the emission bands in fluorescence spectra, both of them included in the term *solvatochromism*, or *solvatofluorchromism* for the last phenomena and generally, dye molecules with high conjugation and polarity, especially with intramolecular charge-transfer, exhibit a strong solvatochromism [82–84]. This way, the emission spectra of the bis- and mono-squaramides were recorded in six different solvents (acetonitrile (ACN), chloroform, EtOH, hexane, tetrahydrofurane (THF) and toluene (TOL)) and the photophysical data are represented in Figure 14. It can be noticed that slightly solvatochromism effects (around 50nm, from 750 to 800 nm) occur for all solvents other than the apolar ones (hexane and toluene). Particularly, the methoxy-mono-naphtylsquaramide **SQ-NPh1** (Figure 13a) exhibits red-shifts with all

polar solvents due to the possible stronger intermolecular dipole-dipole interactions between the solvent and the oxygen atom in the methoxy group. In the case of the bis-derivative **SQ-NPh2** (Figure 13b) it is noticed that only in EtOH and THF the larger red-shift to almost 800 nm can be observed, in the other solvents the solvatochromic effect is much less intense. It can be reported that the literature [82,84,85] cites that EtOH and THF can form strong hydrogen bond interactions with considerable solvatochromic effects. Since the determined solid phase structure of the mono- and bis-squaramides (Figures 6 and 9, respectively) present very intense intermolecular hydrogen bond interactions, the more polar and protic, or hydrogen bond accepting, solvents can diminish the chromophore aggregation and change the energies in the fluorescence phenomena (as described elsewhere, for other very efficient NIR fluorophores [6].This might happen even more intensively for the methoxy-mono-naphtylsquaramide **SQ-NPh1** that can form stronger hydrogen interactions due to the oxygen atom in the methoxy group. Interestingly, the observed solvatochromism effect indeed indicates possible intramolecular charge transfer (ICT), but in a much lower level than expected and this can be explained, especially for the bis-squaramide **SQ-NPh2**, due to its nonplanar molecular structure, as ever reported before by Kosower and co-workers [86–89] about the slightly solvent-dependent fluorescence in the nonplanar molecular system for 6-(arylamino)-2-naphtalene sulfonates. More recently, in 2017, Yang and co- [90] also noticed that maximal absorption wavelength is essentially independent of the nature of solvent for some substituted 10-phenyl-spiro-quinolizino-pentaceno-quinolizine-xanthenium chorides due to their molecular non-planarities and very bulky structures.

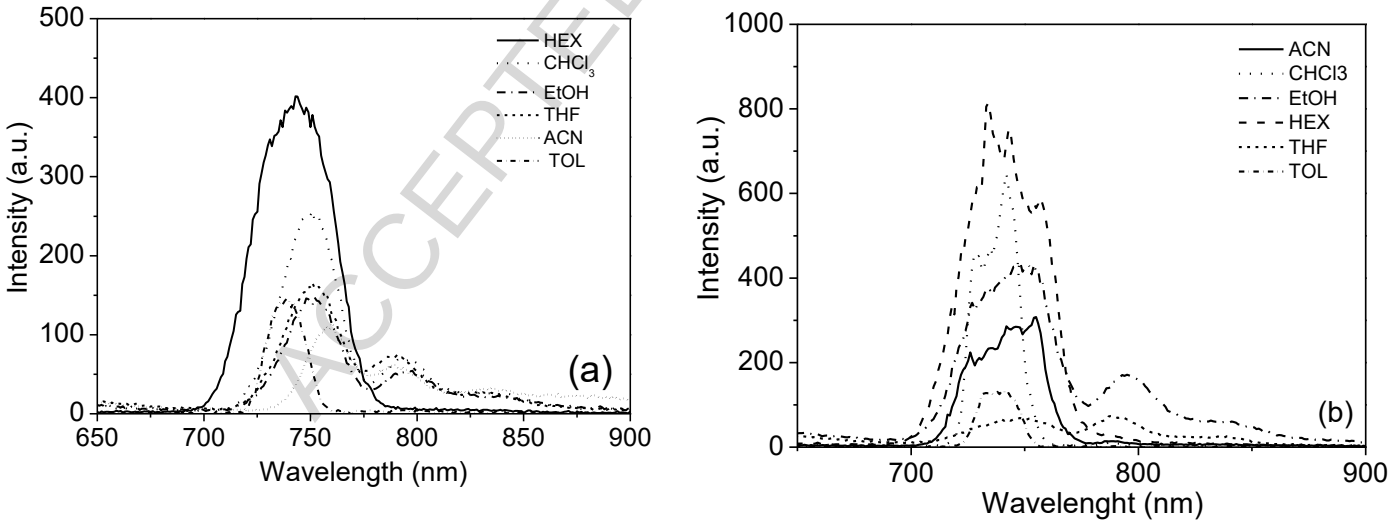

Fig. 13. Fluorescence spectra of a) **SQ-NPh1** and b) **SQ-NPh2**.

4. Conclusions

The present study corroborates that squaric derivatives, electron-acceptor moieties (**A**), really are useful building blocks to obtain novel near-infrared fluorophores, since their functionalization with electron-donating

amines can yield squaramides with a well-known **D-A** molecular architecture that is suitable for the design of novel NIR-emitting agents. The novel mono-methoxy-mono-aminonaphthylsquaramide and the corresponding bis-naphthylsquaramide can be selectively obtained through the condensation of dimethylsquarate in methanol, with different amine/squarate ratios. The actual molecular structure characterization of the obtained mono-squaramide was achieved by ^{13}C-NMR, vibrational spectroscopy (IR and Raman), by X-ray crystallography and by powder diffraction *state-of-art*. These are the first reported squaramides with fluorescent emissions in NIR, at 780 nm for the mono-derivative and 800 nm for the bis-derivative. Additionally, these new NIR fluorescent dyes present quite thermal stability and they might be used as highly stable advanced photochemical material.

Acknowledgments

We are grateful to FAPEMIG (CEX PPM 281-17 and APQ-02715-14) for finantial support and this study was financed in part by the Coordenação de Aperfeiçoamento de Pessoal de Nível Superior-Brasil (CAPES)-Finance Code 001 (INCT-MIDAS). We gratefully acknowledge to CNPq, CAPES and FAPEMIG for scholarships. This work is a collaboration research project of members of the Rede Mineira de Química (RQ-MG) partially supported by CNPq and FAPEMIG.

Reference

[1] Y. Zhang, Y. Wang, J. Song, J. Qu, B. Li, W. Zhu, W.Y. Wong, Near-Infrared Emitting Materials via Harvesting Triplet Excitons: Molecular Design, Properties, and Application in Organic Light Emitting Diodes, Adv. Opt. Mater. 6 (2018) 1–19. doi:10.1002/adom.201800466.

[2] H. Xiang, J. Cheng, X. Ma, X. Zhou, J.J. Chruma, Near-infrared phosphorescence: Materials and applications, 2013. doi:10.1039/c3cs60029g.

[3] G. Qian, Z.Y. Wang, Near-infrared organic compounds and emerging applications, Chem. - An Asian J. 5 (2010) 1006–1029. doi:10.1002/asia.200900596.

[4] A. Haque, M.S.H. Faizi, J.A. Rather, M.S. Khan, Next generation NIR fluorophores for tumor imaging and fluorescence-guided surgery: A review, Bioorganic Med. Chem. 25 (2017) 2017–2034. doi:10.1016/j.bmc.2017.02.061.

[5] Z.Y. Wang, Near-infrared organic materials and emerging applications, CRC press, 2013.

[6] G. Qian, Z. Zhong, M. Luo, D. Yu, Z. Zhang, Z.Y. Wang, D. Ma, Simple and efficient near-infrared organic chromophores for light-emitting diodes with single electroluminescent emission above 1000 nm, Adv. Mater. 21 (2009) 111–116. doi:10.1002/adma.200801918.

[7] S. Tang, P. Murto, X. Xu, C. Larsen, E. Wang, L. Edman, Intense and Stable Near-Infrared Emission from Light-Emitting Electrochemical Cells Comprising a Metal-Free Indacenodithieno[3,2-b]thiophene-Based Copolymer as the Single Emitter, Chem. Mater. 29 (2017) 7750–7759. doi:10.1021/acs.chemmater.7b02049.

[8] P. Murto, S. Tang, C. Larsen, X. Xu, A. Sandström, J. Pietarinen, B. Bagemihl, B.A. Abdulahi, W. Mammo, M.R. Andersson, E. Wang, L. Edman, Incorporation of Designed Donor–Acceptor–Donor Segments in a Host Polymer for Strong Near-Infrared Emission from a Large-Area Light-Emitting Electrochemical Cell, ACS Appl. Energy Mater. 1 (2018) 1753–1761. doi:10.1021/acsaem.8b00283.

[9] M. Koppe, H.J. Egelhaaf, G. Dennler, M.C. Scharber, C.J. Brabec, P. Schilinsky, C.N. Hoth, Near IR sensitization of organic bulk heterojunction solar cells: Towards optimization of the spectral response of organic solar cells, Adv. Funct. Mater. 20 (2010) 338–346. doi:10.1002/adfm.200901473.

[10] H. Chen, B. Dong, Y. Tang, W. Lin, A Unique “integration” Strategy for the Rational Design of Optically Tunable Near-Infrared Fluorophores, Acc. Chem. Res. 50 (2017) 1410–1422. doi:10.1021/acs.accounts.7b00087.

[11] L. Yuan, W. Lin, S. Zhao, W. Gao, B. Chen, L. He, S. Zhu, A Unique Approach to Development of Near-Infrared Fluorescent Sensors for in Vivo Imaging, J. Am. Chem. Soc. 134 (2012) 13510–13523. doi:10.1021/ja305802v.

[12] K.S. Schanze, J.R. Reynolds, J.M. Boncella, B.S. Harrison, T.J. Foley, M. Bouguettaya, T.-S. Kang, Near-infrared organic light emitting diodes, Synth. Met. 137 (2003) 1013–1014. doi:https://doi.org/10.1016/S0379-6779(02)00862-7.

[13] Z. Yang, Y. Yuan, R. Jiang, N. Fu, X. Lu, C. Tian, W. Hu, Q. Fan, W. Huang, Homogeneous near-infrared emissive polymeric nanoparticles based on amphiphilic diblock copolymers with perylene diimide and PEG pendants: self-assembly behavior and cellular imaging application, Polym. Chem. 5 (2014) 1372–1380. doi:10.1039/C3PY01197F.

[14] Y. Ni, J. Wu, Far-red and near infrared BODIPY dyes: synthesis and applications for fluorescent pH probes and bio-imaging, Org. Biomol. Chem. 12 (2014) 3774–3791. doi:10.1039/C3OB42554A.

[15] A.B. Tamayo, B.D. Alleyne, P.I. Djurovich, S. Lamansky, I. Tsyba, N.N. Ho, R. Bau, M.E. Thompson, Synthesis and Characterization of Facial and Meridional Tris-cyclometalated Iridium(III) Complexes, J. Am. Chem. Soc. 125 (2003) 7377–7387. doi:10.1021/ja034537z.

[16] S. Lamansky, P. Djurovich, D. Murphy, F. Abdel-Razzaq, H.-E. Lee, C. Adachi, P.E. Burrows, S.R. Forrest, M.E. Thompson, Highly Phosphorescent Bis-Cyclometalated Iridium Complexes: Synthesis, Photophysical Characterization, and Use in Organic Light Emitting Diodes, J. Am. Chem. Soc. 123 (2001) 4304–4312. doi:10.1021/ja003693s.

[17] J. Brooks, Y. Babayan, S. Lamansky, P.I. Djurovich, I. Tsyba, R. Bau, M.E. Thompson, Synthesis and Characterization of Phosphorescent Cyclometalated Platinum Complexes, Inorg. Chem. 41 (2002) 3055–3066. doi:10.1021/ic0255508.

[18] N.G. Pschirer, C. Kohl, F. Nolde, J. Qu, K. Müllen, Pentarylene- and hexarylenebis(dicarboximide)s: Near-infrared-absorbing polyaromatic dyes, Angew. Chemie - Int. Ed. 45 (2006) 1401–1404. doi:10.1002/anie.200502998.

[19] L. Zhou, Y. Feng, J. Cheng, N. Sun, X. Zhou, H. Xiang, Simple, selective, and sensitive colorimetric and ratiometric fluorescence/phosphorescence probes for platinum(ii) based on Salen-type Schiff bases, RSC Adv. 2 (2012) 10529–10536. doi:10.1039/C2RA21254D.

[20] W. Lu, B.-X. Mi, M.C.W. Chan, Z. Hui, C.-M. Che, N. Zhu, S.-T. Lee, Light-Emitting Tridentate Cyclometalated Platinum(II) Complexes Containing σ-Alkynyl Auxiliaries: Tuning of Photo- and Electrophosphorescence, J. Am. Chem. Soc. 126 (2004) 4958–4971. doi:10.1021/ja0317776.

[21] G. Qian, Z. Zhong, M. Luo, D. Yu, Z. Zhang, D. Ma, Z.Y. Wang, Synthesis and Application of Thiadiazoloquinoxaline-Containing Chromophores as Dopants for Efficient Near-Infrared Organic Light-Emitting Diodes, J. Phys. Chem. C. 113 (2009) 1589–1595. doi:10.1021/jp809568a.

[22] Y. Yang, R.T. Farley, T.T. Steckler, S.H. Eom, J.R. Reynolds, K.S. Schanze, J. Xue, Efficient near-infrared organic light-emitting devices based on low-gap fluorescent oligomers, J. Appl. Phys. 106 (2009). doi:10.1063/1.3204947.

[23] S. Ellinger, K.R. Graham, P. Shi, R.T. Farley, T.T. Steckler, R.N. Brookins, P. Taranekar, J. Mei, L.A. Padilha, T.R. Ensley, H. Hu, S. Webster, D.J. Hagan, E.W. Van Stryland, K.S. Schanze, J.R. Reynolds, Donor–Acceptor–Donor-based π-Conjugated Oligomers for Nonlinear Optics and Near-IR Emission, Chem. Mater. 23 (2011) 3805–3817. doi:10.1021/cm201424a.

[24] Y. Zhang, F. Meng, C. You, S. Yang, W. Xiong, Y. Wang, S. Su, W. Zhu, Achieving NIR emission for tetradentate platinum (II) salophen complexes by attaching dual donor-accepter frameworks in the heads of salophen, Dye. Pigment. 138 (2017) 100–106. doi:10.1016/j.dyepig.2016.11.034.

[25] Y.-M. Zhang, F. Meng, J.-H. Tang, Y. Wang, C. You, H. Tan, Y. Liu, Y.-W. Zhong, S. Su, W. Zhu, Achieving near-infrared emission in platinum(ii) complexes by using an extended donor–acceptor-type ligand, Dalt. Trans. 45 (2016) 5071–5080. doi:10.1039/C5DT04793E.

[26] J. Yu, H. Tan, F. Meng, K. Lv, W. Zhu, S. Su, Benzotriazole-containing donor-acceptor-acceptor type cyclometalated iridium(III) complex for solution-processed near-infrared polymer light emitting diodes, Dye. Pigment. 131 (2016) 231–238. doi:10.1016/j.dyepig.2016.04.021.

[27] J. Yu, K. He, Y. Li, H. Tan, M. Zhu, Y. Wang, Y. Liu, W. Zhu, H. Wu, A novel near-infrared-emitting cyclometalated platinum (II) complex with donor-acceptor-acceptor chromophores, Dye. Pigment. 107 (2014) 146–152. doi:10.1016/j.dyepig.2014.03.040.

[28] A. Ajayaghosh, Donor-acceptor type low band gap polymers: Polysquaraines and related systems, Chem. Soc. Rev. 32 (2003) 181–191. doi:10.1039/b204251g.

[29] J. Chen, R.F. Winter, Studies on a vinyl ruthenium-modified squaraine dye: Multiple visible/near-infrared absorbance switching through dye- and substituent-based redox processes, Chem. - A Eur. J. 18 (2012) 10733–10741. doi:10.1002/chem.201200800.

[30] A.H. Schmidt, Reaktionen von Quadratsäure und Quadratsäure-Derivaten, Synthesis (Stuttg). 1980 (1980) 961–994. doi:10.1055/s-1980-29291.

[31] R. Ian Storer, C. Aciro, L.H. Jones, Squaramides: Physical properties, synthesis and applications, Chem. Soc. Rev. 40 (2011) 2330–2346. doi:10.1039/c0cs00200c.

[32] F.R. Wurm, H.A. Klok, Be squared: Expanding the horizon of squaric acid-mediated conjugations, Chem. Soc. Rev. 42 (2013) 8220–8236. doi:10.1039/c3cs60153f.

[33] L.F.C. De Oliveira, S.R. Mutareuj, N.S. Gonçalves, Estrutura E Espectroscopia Vibracional De Oxocarbonos E De Suas Espécies De Coordenação, Quim. Nova. 15 (1992).

[34] L.F. Tietze, M. Arlt, M. Beller, K. -H Gl üsenkamp, E. Jähde, M.F. Rajewsky, Anticancer Agents, 15. Squaric Acid Diethyl Ester: A New Coupling Reagent for the Formation of Drug Biopolymer Conjugates. Synthesis of Squaric Acid Ester Amides and Diamides, Chem. Ber. 124 (1991) 1215–1221.

doi:10.1002/cber.19911240539.
[35] E.W. Neuse, B.R. Green, Dianilino Derivatives of Squaric Acid, J. Org. Chem. 39 (1974) 3881–3887. doi:10.1021/jo00940a018.
[36] S. Sreejith, P. Carol, P. Chithra, A. Ajayaghosh, Squaraine dyes: A mine of molecular materials, J. Mater. Chem. 18 (2008) 264–274. doi:10.1039/b707734c.
[37] S.-W. Duan, Y. Li, Y.-Y. Liu, Y.-Q. Zou, D.-Q. Shi, W.-J. Xiao, An organocatalytic Michael-aldol cascade: formal [3+2] annulation to construct enantioenriched spirocyclic oxindole derivatives, Chem. Commun. 48 (2012) 5160–5162. doi:10.1039/C2CC30931A.
[38] J.P. Malerich, K. Hagihara, V.H. Rawal, Chiral squaramide derivatives are excellent hydrogen bond donor catalysts, J. Am. Chem. Soc. 130 (2008) 14416–14417. doi:10.1021/ja805693p.
[39] X. Han, H. Zhou, C. Dong, Applications of Chiral Squaramides : From Asymmetric Organocatalysis to Biologically Active Compounds, (2016) 897–906. doi:10.1002/tcr.201500266.
[40] S.H. Kim, J.H. Kim, J.Z. Cui, Y.S. Gal, S.H. Jin, K. Koh, Absorption spectra, aggregation and photofading behaviour of near-infrared absorbing squarylium dyes containing perimidine moiety, Dye. Pigment. 55 (2002) 1–7. doi:10.1016/S0143-7208(02)00051-7.
[41] A.C. Tam, Optoacoustic determination of photocarrier generation efficiencies of dye films, Appl. Phys. Lett. 37 (1980) 978–981. doi:10.1063/1.91725.
[42] S.F. Völker, M. Renz, M. Kaupp, C. Lambert, Squaraine dyes as efficient coupling bridges between triarylamine redox centres, Chem. - A Eur. J. 17 (2011) 14147–14163. doi:10.1002/chem.201102227.
[43] S. Yagi, H. Nakazumi, Squarylium Dyes and Related Compounds, Heterocycl. Polymethine Dye. (2008) 133–181. doi:10.1007/7081_2008_117.
[44] L. Beverina, P. Salice, Squaraine compounds: Tailored design and synthesis towards a variety of material science applications, European J. Org. Chem. (2010) 1207–1225. doi:10.1002/ejoc.200901297.
[45] F.P. Gao, Y.X. Lin, L.L. Li, Y. Liu, U. Mayerhöffer, P. Spenst, J.G. Su, J.Y. Li, F. Würthner, H. Wang, Supramolecular adducts of squaraine and protein for noninvasive tumor imaging and photothermal therapy invivo, Biomaterials. 35 (2014) 1004–1014. doi:10.1016/j.biomaterials.2013.10.039.
[46] C.C. Defilippo, H. Tang, L. Ravotto, G. Bergamini, P. Salice, M. Mba, P. Ceroni, E. Galoppini, M. Maggini, Synthesis and electronic properties of 1,2-hemisquarimines and their encapsulation in a cucurbit[7]uril host, Chem. - A Eur. J. 20 (2014) 6412–6420. doi:10.1002/chem.201400039.
[47] P. Salice, E. Ronchi, A. Iacchetti, M. Binda, D. Natali, W. Gomulya, M. Manca, M.A. Loi, M. Iurlo, F. Paolucci, M. Maggini, G.A. Pagani, L. Beverina, E. Menna, A fulleropyrrolidine-squaraine blue dyad: Synthesis and application as an organic light detector, J. Mater. Chem. C. 2 (2014) 1396–1399. doi:10.1039/c3tc32205j.
[48] X.M. Yi, F.L. Wang, W.J. Qin, X.J. Yang, J.L. Yuan, Near-infrared fluorescent probes in cancer imaging and therapy: An emerging field, Int. J. Nanomedicine. 9 (2014) 1347–1365. doi:10.2147/IJN.S60206.
[49] Rigaku Corporation, (2015).
[50] G.M. Sheldrick, Crystal structure refinement with SHELXL, Acta Crystallogr. Sect. C Struct. Chem. 71 (2015) 3–8. doi:10.1107/S2053229614024218.
[51] L.J. Farrugia, ORTEP-3 for Windows-a version of ORTEP-III with a Graphical User Interface (GUI), J. Appl. Crystallogr. 30 (1997) 565.
[52] C.F. Macrae, I.J. Bruno, J.A. Chisholm, P.R. Edgington, P. McCabe, E. Pidcock, L. Rodriguez-Monge, R. Taylor, J. van de Streek, P.A. Wood, Mercury CSD 2.0–new features for the visualization and investigation of crystal structures, J. Appl. Crystallogr. 41 (2008) 466–470.
[53] A.A. Coelho, Indexing of powder diffraction patterns by iterative use of singular value decomposition, J. Appl. Crystallogr. 36 (2003) 86–95.
[54] U. Manual, V. TOPAS, 0: General profile and structure analysis software for powder diffraction data, Karlsruhe, Ger. (2000).
[55] G. Pawley, Unit-cell refinement from powder diffraction scans, J. Appl. Crystallogr. 14 (1981) 357–361. https://doi.org/10.1107/S0021889881009618.
[56] A. Spek, Structure validation in chemical crystallography, Acta Crystallogr. Sect. D. 65 (2009) 148–155.

https://doi.org/10.1107/S090744490804362X.
[57] A. Coelho, Whole-profile structure solution from powder diffraction data using simulated annealing, J. Appl. Crystallogr. 33 (2000) 899–908. https://doi.org/10.1107/S002188980000248X.
[58] M.C. Melquíades, R. Aderne, A. Cuin, W.G. Quirino, M. Cremona, C. Legnani, Investigation of Tin(II)2,3-naphtalocyanine molecule used as near-infrared sensitive layer in organic up-conversion devices, Opt. Mater. (Amst). 69 (2017) 54–60. doi:https://doi.org/10.1016/j.optmat.2017.04.018.
[59] S.A. Silva, N. Masciocchi, A. Cuin, Crystal structures of N,N′-bis(thiophen-2-ylmethyl)ethane-1,2-diaminium hydrochloride and of its [AuCl4]− salt solved by powder diffraction, Powder Diffr. 29 (2014) 300–306. doi:DOI: 10.1017/S0885715614000530.
[60] T.C. Amaral, F.B. Miguel, M.R.C. Couri, P.P. Corbi, M.A. Carvalho, D.L. Campos, F.R. Pavan, A. Cuin, Silver(I) and zinc(II) complexes with symmetrical cinnamaldehyde Schiff base derivative: Spectroscopic, powder diffraction characterization, and antimycobacterial studies, Polyhedron. 146 (2018) 166–171. doi:https://doi.org/10.1016/j.poly.2018.02.024.
[61] D. Cox, The Rietveld method. (IUCr Monograph on Crystallography, No. 5) edited by R. A. Young, J. Appl. Crystallogr. 27 (1994) 440–441. https://doi.org/10.1107/S0021889894000439.
[62] S. Sopeña, E. Martin, E.C. Escudero-Adán, A.W. Kleij, Pushing the Limits with Squaramide-Based Organocatalysts in Cyclic Carbonate Synthesis, ACS Catal. 7 (2017) 3532–3539. doi:10.1021/acscatal.7b00475.
[63] H. Liu, C.S. Tomooka, H.W. Moore, An efficient general synthesis of squarate esters, Synth. Commun. 27 (1997) 2177–2180. doi:10.1080/00397919708006826.
[64] C. López, M. Vega, E. Sanna, C. Rotger, A. Costa, Efficient microwave-assisted preparation of squaric acid monoamides in water, RSC Adv. 3 (2013) 7249–7253. doi:10.1039/c3ra41369a.
[65] M. Chavez-Castillo, A. Ledesma-Juarez, M. Guizado-Rodriguez, J. Castrellon-Uribe, G. Ramos-Ortiz, M. Rodríguez, J.L. Maldonado, J.A. Guerrero-Alvarez, V. Barba, Third-order nonlinear optical behavior of novel polythiophene derivatives functionalized with disperse red 19 chromophore, Int. J. Polym. Sci. 2015 (2015). doi:10.1155/2015/219361.
[66] J. Xie, A.B. Comeau, C.T. Seto, Squaric Acids: A New Motif for Designing Inhibitors of Protein Tyrosine Phosphatases, Org. Lett. 6 (2004) 83–86. doi:10.1021/ol036121w.
[67] G. Xia, C. Ruan, H. Wang, Highly sensitive detection of carbon dioxide by a pyrimido[1,2-a]benzimidazole derivative: combining experimental and theoretical studies, Analyst. 140 (2015) 5099–5104. doi:10.1039/C5AN00947B.
[68] A. V Ivachtchenko, Synthesis of the Substituted 3-Cyclobutene-, (2007) 2527–2542. doi:10.1080/00397910701462716.
[69] C. Prabhakar, K. Bhanuprakash, V.J. Rao, M. Balamuralikrishna, D.N. Rao, Third order nonlinear optical properties of squaraine dyes having absorption below 500 nm: A combined experimental and theoretical investigation of closed shell oxyallyl derivatives, J. Phys. Chem. C. 114 (2010) 6077–6089. doi:10.1021/jp908475n.
[70] M.C. Rotger, M.N. Piña, A. Frontera, G. Martorell, P. Ballester, P.M. Deyà, A. Costa, Conformational Preferences and Self-Template Macrocyclization of Squaramide-Based Foldable Modules, J. Org. Chem. 69 (2004) 2302–2308. doi:10.1021/jo035546t.
[71] A. Ranganathan, G.U. Kulkarni, An Experimental Electron Density Investigation of Squarate and Croconate Dianions, J. Phys. Chem. A. 106 (2002) 7813–7819. doi:10.1021/jp013902a.
[72] C.E. Silva, H.F. Dos Santos, N.L. Speziali, R. Diniz, L.F.C. de Oliveira, Role of the Substituent Effect over the Squarate Oxocarbonic Ring: Spectroscopy, Crystal Structure, and Density Functional Theory Calculations of 1,2-Dianilinosquairane, J. Phys. Chem. A. 114 (2010) 10097–10109. doi:10.1021/jp105346h.
[73] C. Rotger, B. Soberats, D. Quiñonero, A. Frontera, P. Ballester, J. Benet-Buchholz, P.M. Deyà, A. Costa, Crystallographic and Theoretical Evidence of Anion–π and Hydrogen-Bonding Interactions in a Squaramide–Nitrate Salt, European J. Org. Chem. 2008 (2008) 1864–1868. doi:10.1002/ejoc.200701209.
[74] D. Braga, L. Maini, F. Grepioni, Croconic Acid and Alkali Metal Croconate Salts: Some New Insights

into an Old Story, Chem. – A Eur. J. 8 (2002) 1804–1812. doi:10.1002/1521-3765(20020415)8:8<1804::AID-CHEM1804>3.0.CO;2-C.

[75] A. P. Davis, S. M. Draper, G. Dunne, P. Ashton, The N-carbamoyl squaramide dimer: a compact, strongly associated H-bonding motif, Chem. Commun. (1999) 2265–2266. doi:10.1039/A907179B.

[76] A. Portell, R. Barbas, D. Braga, M. Polito, C. Puigjaner, R. Prohens, New polymorphic hydrogen bonding donor–acceptor system with two temperature coincident solid–solid transitions, CrystEngComm. 11 (2009) 52–54. doi:10.1039/B813086H.

[77] E. Keller, Neues von SCHAKAL, Chemie Unserer Zeit. 20 (1986) 178–181. doi:10.1002/ciuz.19860200603.

[78] U. Mayerhöffer, B. Fimmel, F. Würthner, Bright near-infrared fluorophores based on squaraines by unexpected halogen effects, Angew. Chemie - Int. Ed. 51 (2012) 164–167. doi:10.1002/anie.201107176.

[79] G. Chen, H. Sasabe, T. Igarashi, Z. Hong, J. Kido, Squaraine dyes for organic photovoltaic cells, J. Mater. Chem. A. 3 (2015) 14517–14534. doi:10.1039/C5TA01879J.

[80] S. Yagi, T. Ohta, N. Akagi, H. Nakazumi, The synthesis and optical properties of bis-squarylium dyes bearing arene and thiophene spacers, 77 (2008). doi:10.1016/j.dyepig.2007.08.002.

[81] A. Hantzsch, Über die Halochromie und »Solvatochromie« des Dibenzal-acetons und einfacherer Ketone, sowie ihrer Ketochloride, Berichte Der Dtsch. Chem. Gesellschaft (A B Ser. 55 (1922) 953–979. doi:10.1002/cber.19220550420.

[82] C. Reichardt, Solvatochromic Dyes as Solvent Polarity Indicators, Chem. Rev. 94 (1994) 2319–2358. doi:10.1021/cr00032a005.

[83] A.A. Ishchenko, Structure and spectral-luminescent properties of polymethine dyes, Russ. Chem. Rev. 60 (1991) 865.

[84] C. Reichardt, T. Welton, Solvents and solvent effects in organic chemistry, VCH Publishers, 2003.

[85] P. Suppan, Invited review solvatochromic shifts: The influence of the medium on the energy of electronic states, J. Photochem. Photobiol. A Chem. 50 (1990) 293–330. doi:https://doi.org/10.1016/1010-6030(90)87021-3.

[86] E.M. Kosower, H. Dodiuk, K. Tanizawa, M. Ottolenghi, N. Orbach, Intramolecular donor-acceptor systems. Radiative and nonradiative processes for the excited states of 2-N-arylamino-6-naphthalenesulfonates, J. Am. Chem. Soc. 97 (1975) 2167–2178. doi:10.1021/ja00841a030.

[87] E.M. Kosower, Intramolecular donor-acceptor systems. 9. Photophysics of (phenylamino)naphthalenesulfonates: a paradigm for excited-state intramolecular charge transfer, Acc. Chem. Res. 15 (1982) 259–266. doi:10.1021/ar00080a005.

[88] E.M. Kosower, Mechanism of fast intramolecular electron-transfer reactions, J. Am. Chem. Soc. 107 (1985) 1114–1118. doi:10.1021/ja00291a005.

[89] E.M. Kosower, H. Kanety, H. Dodiuk, G. Striker, T. Jovin, H. Boni, D. Huppert, Intramolecular donor-acceptor systems. 7. Solvent dielectric relaxation effects on the photophysics of 6-(phenylamino)-N,N-dimethyl-2-naphthalenesulfonamides, J. Phys. Chem. 87 (1983) 2479–2484. doi:10.1021/j100237a010.

[90] Z. Lei, X. Li, X. Luo, H. He, J. Zheng, X. Qian, Y. Yang, Bright, Stable, and Biocompatible Organic Fluorophores Absorbing/Emitting in the Deep Near-Infrared Spectral Region, Angew. Chemie Int. Ed. 56 (2017) 2979–2983. doi:10.1002/anie.201612301.

Novel Near Infrared Emitter mono-methoxy-mono-naphthyl and di-naphthyl squaramides

High thermal stability for possible applications as novel NIR fluorophore dyes

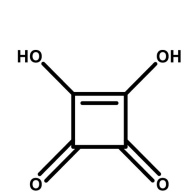

1

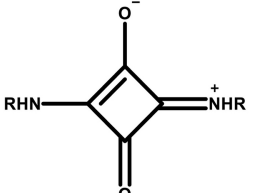

2

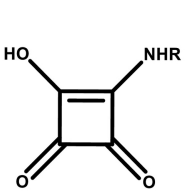

3a

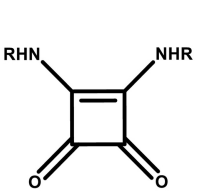

3b

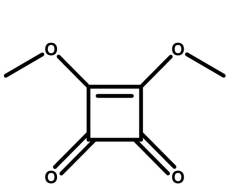

4

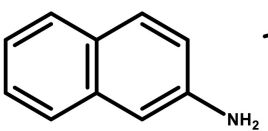

5

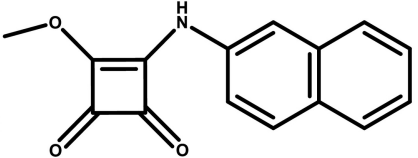

SQ-NPh1

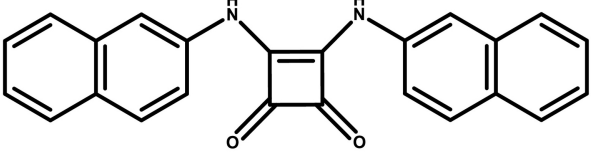

SQ-NPh2

Figure 1

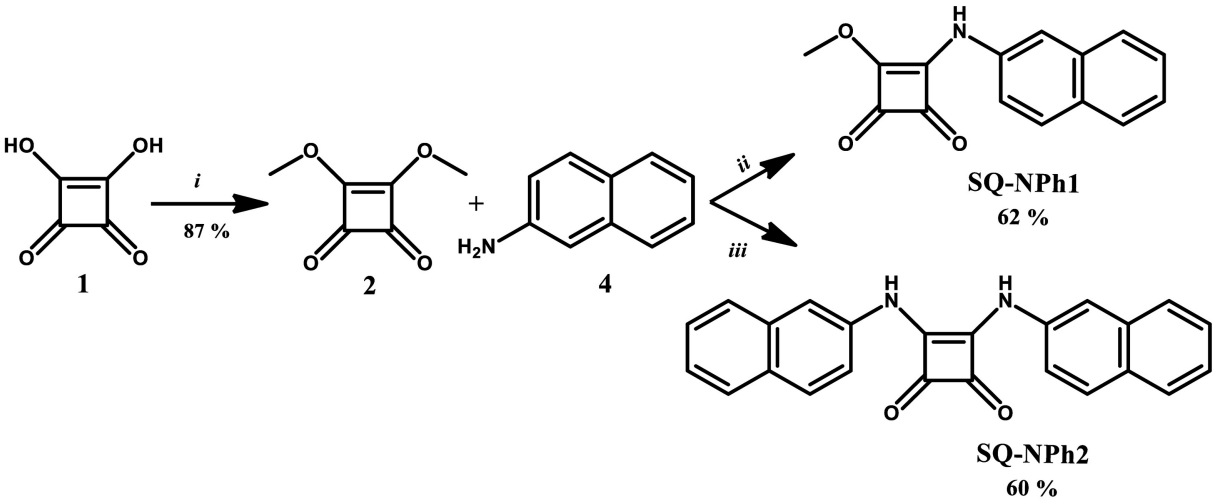

i **= H_2SO_4, MeOH, reflux, 24 h ;** ***ii, iii*** **= MeOH, stirred, 12 h**

Figure 2

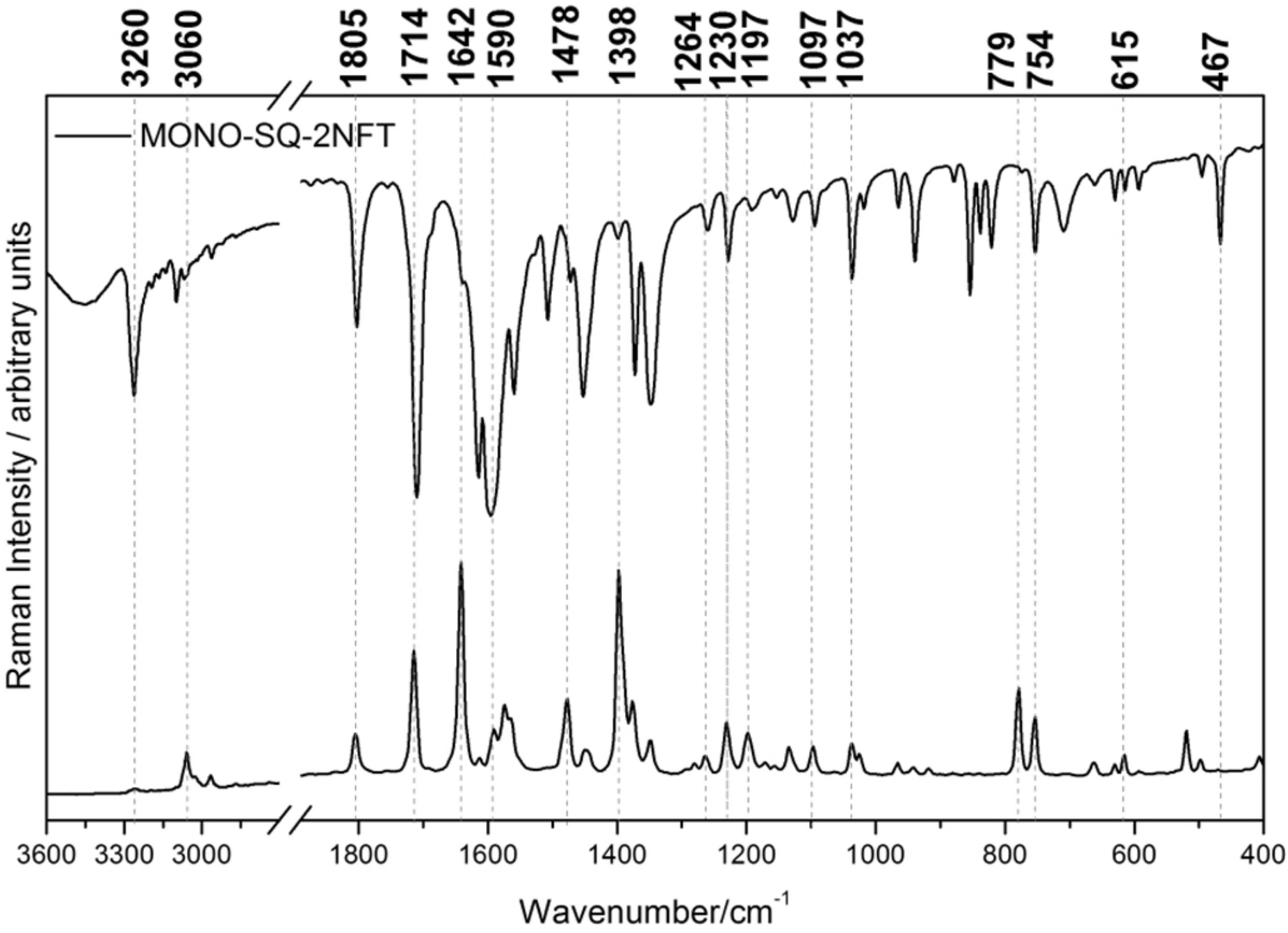
3260
3060
1805
1714
1642
1590
1478
1398
1264
1230
1197
1097
1037
779
754
615
467
MONO-SQ-2NFT
Raman Intensity / arbitrary units
3600
3300
3000
1800
1600
1400
1200
1000
800
600
400
Wavenumber/cm-1

Figure 3

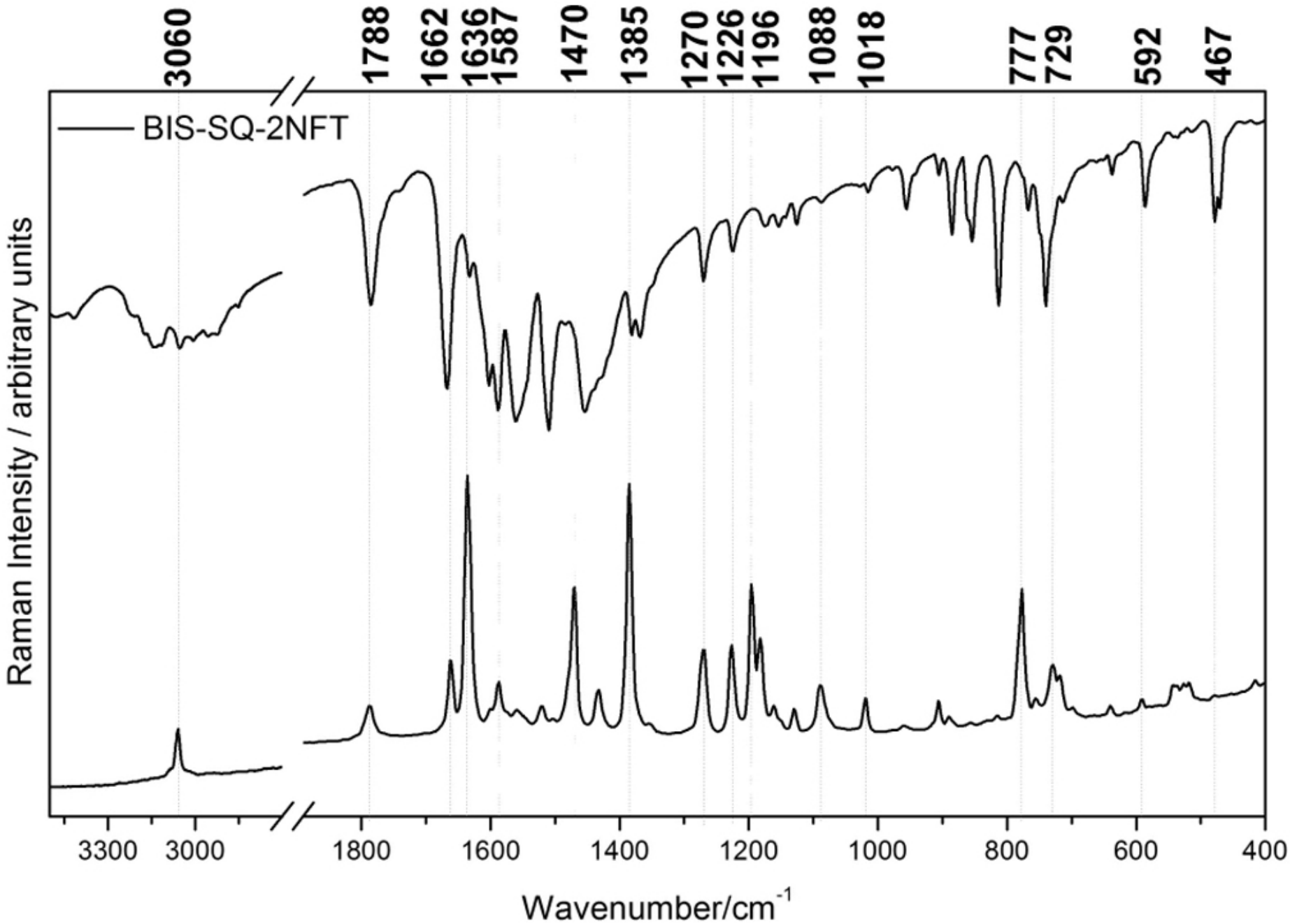
3060
1788
1662
1636
1587
1470
1385
1270
1226
1196
1088
1018
777
729
592
467
BIS-SQ-2NFT
Raman Intensity / arbitrary units
3300
3000
1800
1600
1400
1200
1000
800
600
400
Wavenumber/cm-1

Figure 4

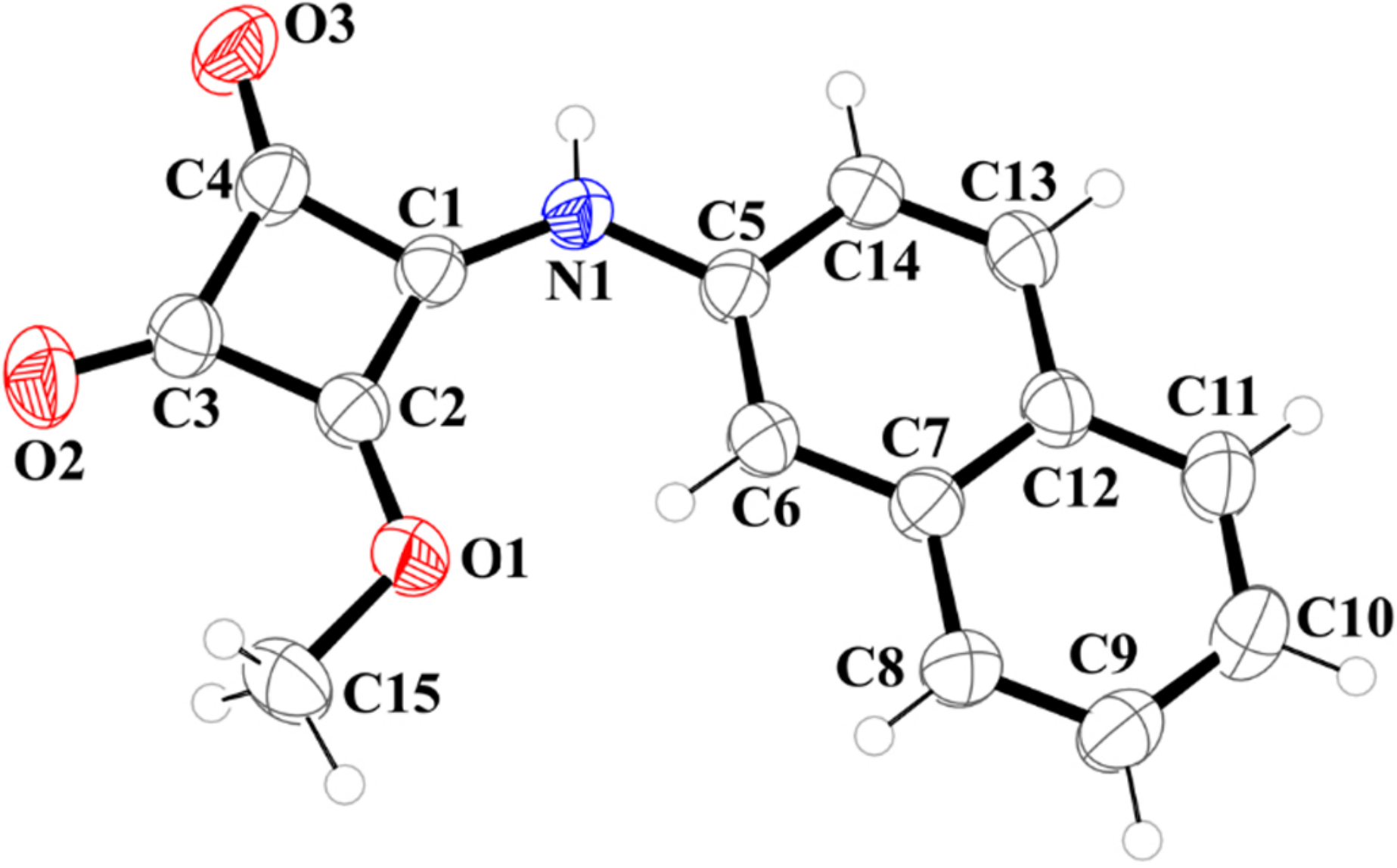

Figure 5

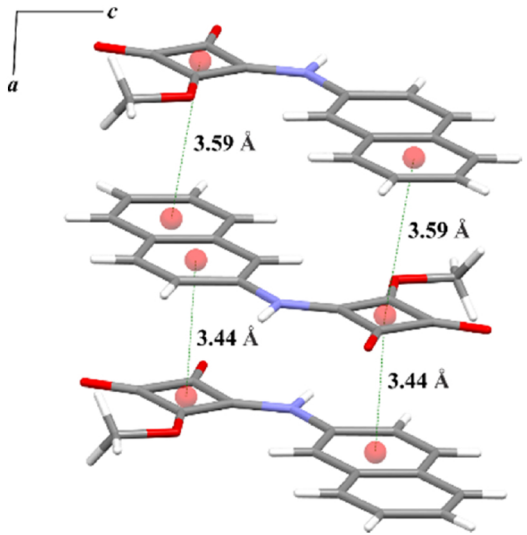

(a)

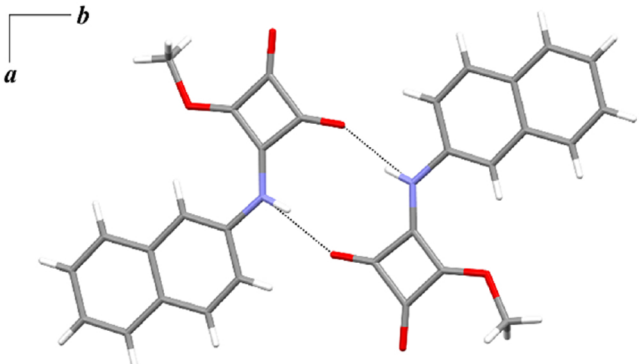

(b)

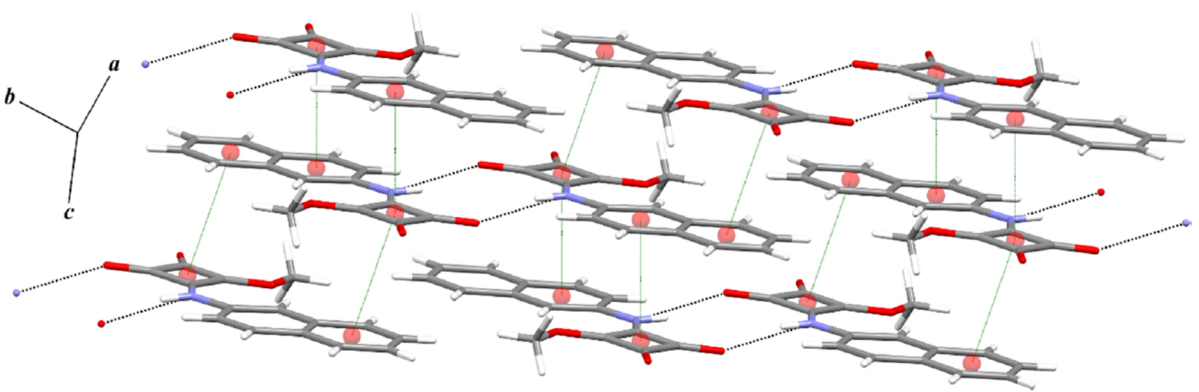

(c)

Figure 6

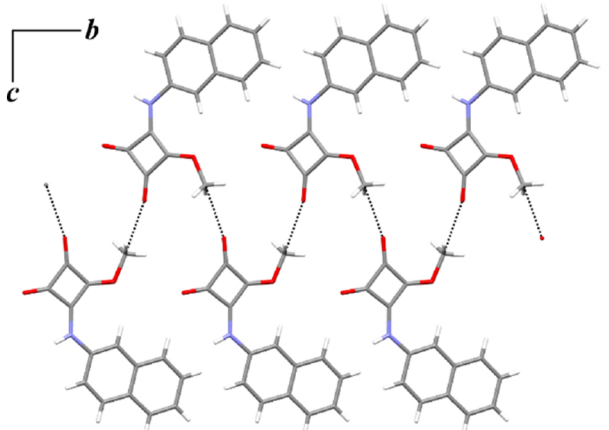

(a)

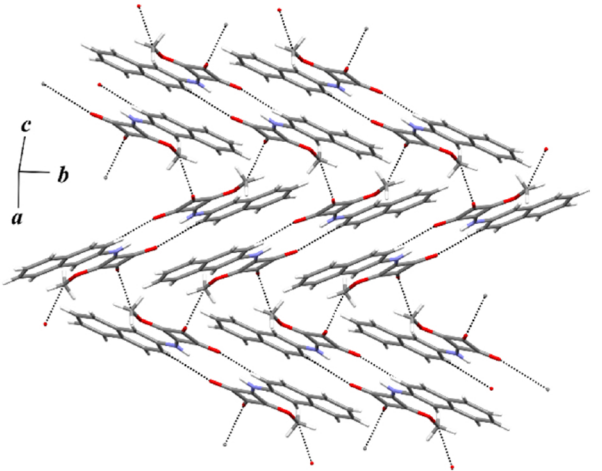

(b)

Figure 7

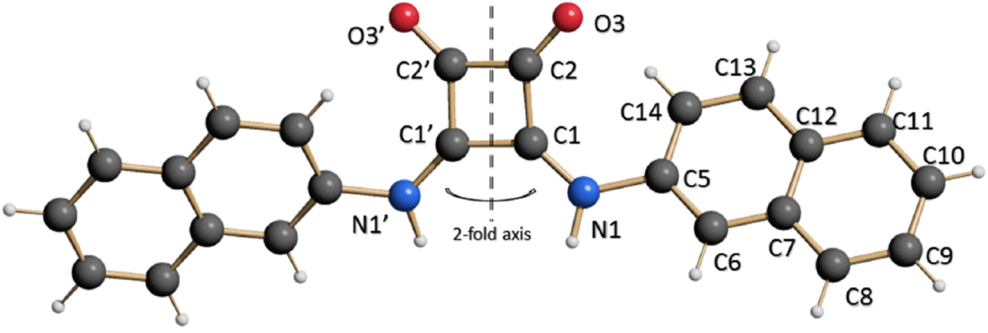
O3'
O3
C2'
C2
C1'
C1
C13
C14
C12
C11
C10
C5
N1'
2-fold axis
N1
C6
C7
C9
C8

Figure 8

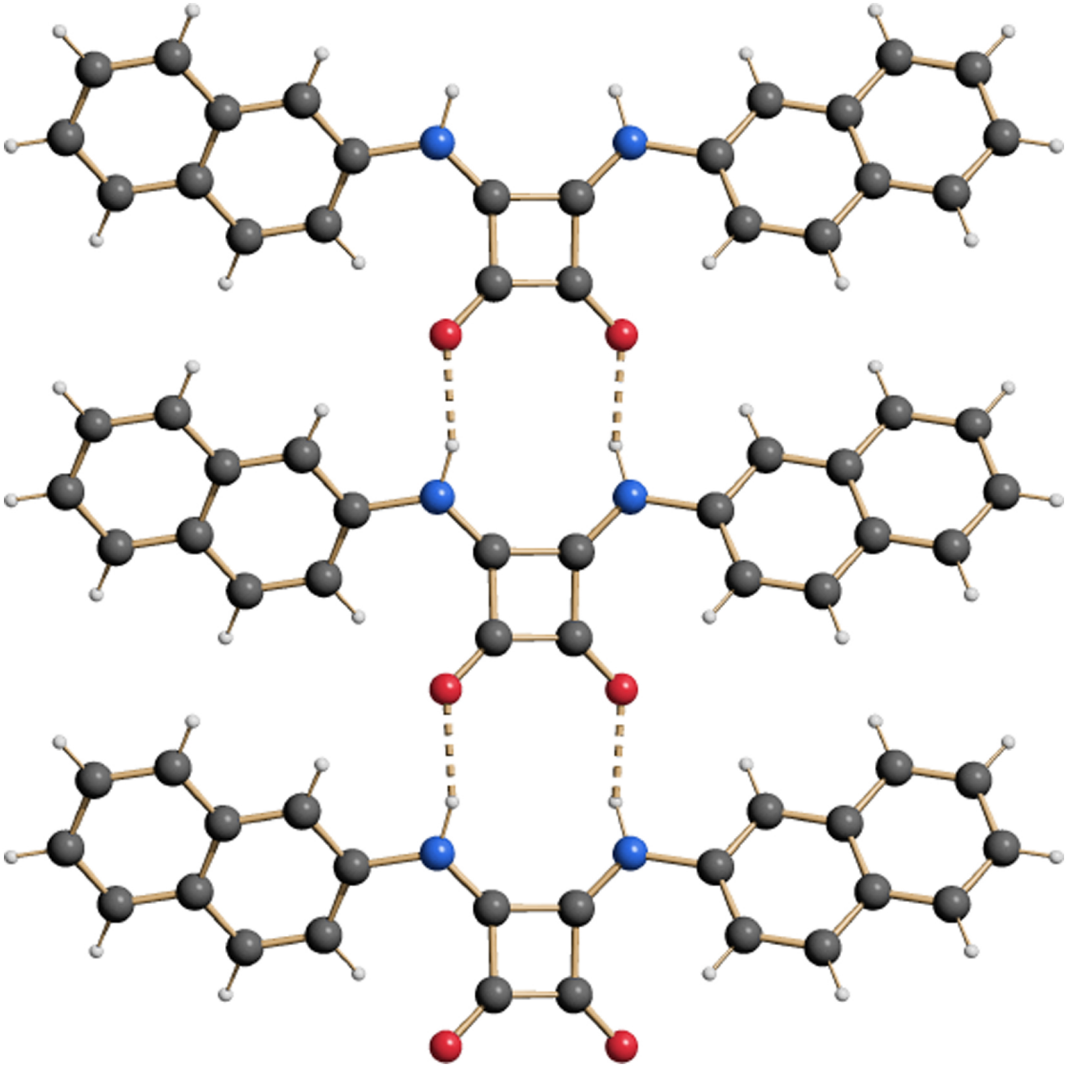

Figure 9

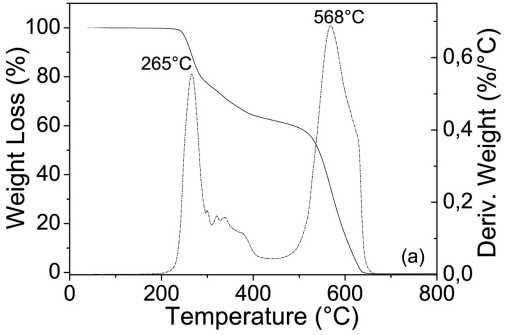
Weight Loss (%)
Deriv. Weight (%/°C)
Temperature (°C)
265°C
568°C
(a)

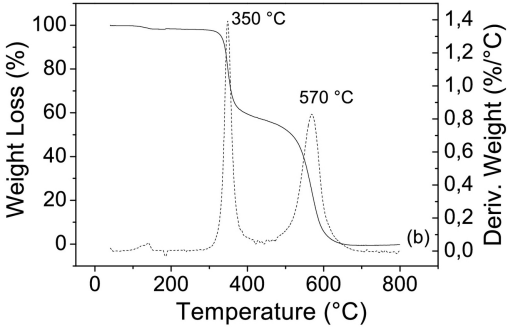
Weight Loss (%)
Deriv. Weight (%/°C)
Temperature (°C)
350 °C
570 °C
(b)

Figure 10

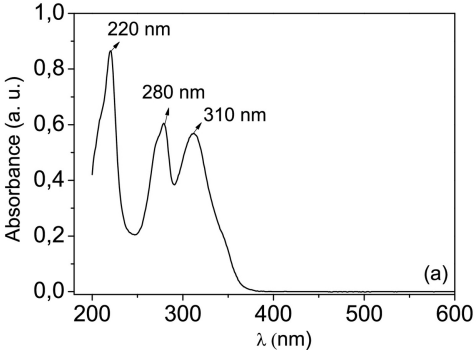
1,0
0,8
0,6
0,4
0,2
0,0
Absorbance (a. u.)
220 nm
280 nm
310 nm
(a)
200
300
400
500
600
λ (nm)

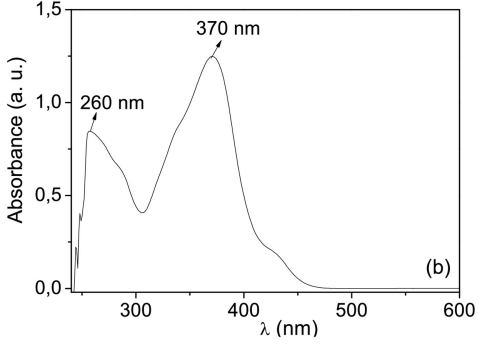
1,5
1,0
0,5
0,0
Absorbance (a. u.)
370 nm
260 nm
(b)
300
400
500
600
λ (nm)

Figure 11

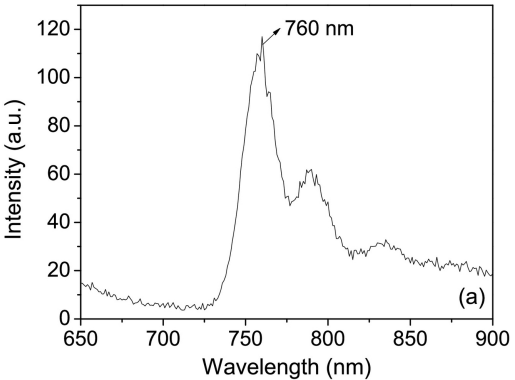
760 nm
Intensity (a.u.)
Wavelength (nm)
(a)
0
20
40
60
80
100
120
650
700
750
800
850
900

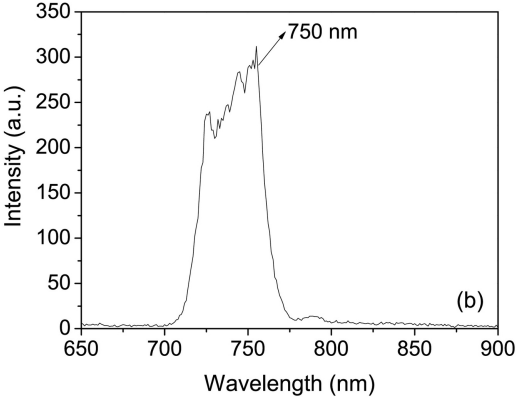
750 nm
Intensity (a.u.)
Wavelength (nm)
(b)
0
50
100
150
200
250
300
350
650
700
750
800
850
900

Figure 12

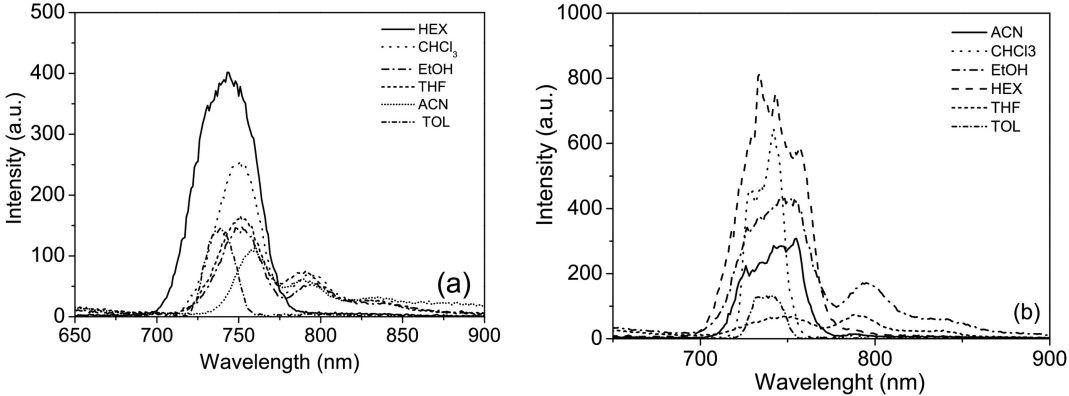
Intensity (a.u.)
Wavelength (nm)
HEX
CHCl3
EtOH
THF
ACN
TOL
(a)
Intensity (a.u.)
Wavelenght (nm)
ACN
CHCl3
EtOH
HEX
THF
TOL
(b)

Figure 13